Plant Physiology and Biochemistry 112 (2017) 346–361

Contents lists available at ScienceDirect

Plant Physiology and Biochemistry

journal homepage: www.elsevier.com/locate/plaphy

Research article

Constitutive heterologous overexpression of a TIR-NB-ARC-LRR gene encoding a putative disease resistance protein from wild Chinese *Vitis pseudoreticulata* in Arabidopsis and tobacco enhances resistance to phytopathogenic fungi and bacteria

Zhifeng Wen [a, b, c], Liping Yao [d], Stacy D. Singer [e], Hanif Muhammad [a, b], Zhi Li [a, b, **], Xiping Wang [a, b, *]

[a] State Key Laboratory of Crop Stress Biology in Arid Areas, College of Horticulture, Northwest A&F University, Yangling, Shaanxi 712100, China
[b] Key Laboratory of Horticultural Plant Biology and Germplasm Innovation in Northwest China, Ministry of Agriculture, Northwest A&F University, Yangling, Shaanxi 712100, China
[c] College of Horticulture, Fujian Agriculture and Forestry University, Fuzhou, Fujian 350002, China
[d] Horticultural Plant Biology and Metabolomics Center, Haixia Institute of Science and Technology, Fujian Agriculture and Forestry University, Fuzhou 350002, China
[e] Department of Agricultural, Food and Nutritional Science, University of Alberta, Edmonton, Alberta T6G 2P5, Canada

ARTICLE INFO

Article history:
Received 30 September 2016
Received in revised form
13 January 2017
Accepted 14 January 2017
Available online 17 January 2017

Keywords:
Wild Chinese *vitis*
VpTNL1
Disease resistance
Powdery mildew
Promoter analysis

ABSTRACT

Plants use resistance (R) proteins to detect pathogen effector proteins and activate their innate immune response against the pathogen. The majority of these proteins contain an NB-ARC (nucleotide-binding adaptor shared by APAF-1, R proteins, and CED-4) domain along with a leucine-rich repeat (LRR), and some also bear a toll interleukin 1 receptor (TIR) domain. In this study, we characterized a gene encoding a TIR-NB-ARC-LRR R protein (VpTNL1) (GenBank accession number KX649890) from wild Chinese grapevine *Vitis pseudoreticulata* accession "Baihe-35-1", which was identified previously from a transcriptomic analysis of leaves inoculated with powdery mildew (PM; *Erysiphe necator* (Schw.)). The *VpTNL1* transcript was found to be highly induced in *V. pseudoreticulata* following inoculation with *E. necator*, as well as treatment with salicylic acid (SA). Sequence analysis demonstrated that the deduced amino acid sequence contained a TIR domain at the N-terminus, along with an NB-ARC and four LRRs domains within the C-terminus. Constitutive expression of *VpTNL1* in *Arabidopsis thaliana* resulted in either a wild-type or dwarf phenotype. Intriguingly, the phenotypically normal transgenic lines displayed enhanced resistance to Arabidopsis PM, *Golovinomyces cichoracearum*, as well as to the virulent bacterial pathogen *Pseudomonas syringae* pv. tomato DC3000. Similarly, constitutive expression of *VpTNL1* in *Nicotiana tabacum* was found to confer enhanced resistance to tobacco PM, *Erysiphe cichoacearum* DC. Subsequent isolation of the *VpTNL1* promoter and deletion analysis indicated that TC-rich repeats and TCA elements likely play an important role in its response to *E. necator* and SA treatment, respectively. Taken together, these results indicate that *VpTNL1* contributes to PM resistance in grapevine and provide an interesting gene target for the future amelioration of grape via breeding and/or biotechnology.

Abbreviations: PRRs, Pattern-recognition receptors; MAMPs, Microbe-associated molecular patterns; PTI, Pattern-triggered immunity; ETI, Effector-triggered immunity; PR1, Pathogenesis-related 1; HR, Hypersensitive response; LRR, Leucine-rich repeat; NB, Nucleotide binding; CC, Coiled-coil; PM, Powdery mildew; SA, Salicylic acid; BA, Benzylaminopurine; IBA, Indole-3-butytric acid; NBT, Nitroblue tetrazolium; hpi, Hours post-inoculation; dpi, Days post-inoculation.

* Corresponding author. College of Horticulture, Northwest A&F University, Yangling 712100, Shaanxi, China.
** Corresponding author. College of Horticulture, Northwest A&F University, Yangling 712100, Shaanxi, China.
E-mail addresses: zhifengwen@126.com (Z. Wen), lpy106080@163.com (L. Yao), stacysinger@hotmail.com (S.D. Singer), mdhanif1716@yahoo.com (H. Muhammad), lizhi@nwsuaf.edu.cn (Z. Li), wangxiping@nwsuaf.edu.cn (X. Wang).

http://dx.doi.org/10.1016/j.plaphy.2017.01.017
0981-9428/

1. Introduction

Plants have evolved two main lines of defense against pathogen infection, the first of which occurs when pattern-recognition receptors (PRRs) detect microbe-associated molecular patterns (MAMPs) (Boller and Felix, 2009) and trigger a downstream defense response known as pattern-triggered immunity (PTI) (Mantelin et al., 2011; Peng and Kaloshian, 2014). To suppress PTI, pathogens have developed specialized secretion systems that deliver effector molecules into the plant cell. In order to overcome these effector molecules, plants have co-evolved to produce resistance (R) proteins, which directly or indirectly recognize pathogen effectors and activate a second line of defense known as effector-triggered immunity (ETI) (Mantelin et al., 2011). ETI typically leads to an active defense response, including the production of pathogenesis-related 1 (PR1) protein, reactive oxygen species (ROS), phytoalexins and hypersensitive response (HR) (Torres et al., 2006; Berger et al., 2007; Ahuja et al., 2012; Peng and Kaloshian, 2014). As such, identifying and investigating the role of R proteins in plant disease resistance can potentially unveil mechanisms underlying R protein/pathogen effector interactions and thus aid in the development of novel treatments to control and prevent pathogen invasion.

The major class of R proteins are structurally conserved with a nucleotide binding (NB) domain and a C-terminal leucine-rich repeat (LRR) domain, known as the NB-LRR protein family (Ooijen et al., 2008), or NB-ARC (for NB adaptor shared by APAF-1, R proteins, and CED-4)-LRR proteins. The three-dimensional structure of these proteins has revealed that the NB-ARC domain, which functions as a molecular switch to regulate signaling pathways through conformational changes (Riedl et al., 2005; Takken et al., 2006; Wen et al., 2015), is composed of four subdomains: the nucleotide-binding (NB) fold and ARC1, -2 and -3 subdomains (Ooijen et al., 2008). Furthermore, several conserved motifs have been identified within this domain, including hhGRExE, Walker A, Walker B, RNBS-A, -B, -C, and -D, GLPL, and MHD motifs (Takken et al., 2006; Ooijen et al., 2008). The LRR domain, on the other hand, is characterized by a LxxLxLxxN/CxL motif (where x can be any amino acid and L denotes valine, isoleucine or phenylalanine) (Kobe and Deisenhofer, 1994; Kajava, 1998) and functions to specifically recognize particular pathogen effectors, providing maintenance in a signaling-competent yet auto-inhibited state (Fenyker et al., 2015).

NB-ARC-LRR proteins can be divided into two classes based on their N-terminal domain, which can comprise either a Toll/interleukin-1 receptor (TIR) domain (TIR-NB-ARC-LRR; TNL family) or a coiled-coil (CC) domain (CC-NB-LRR; CNL family) (Dangl and Jones, 2001; Lukasik-Shreepaathy et al., 2012). TIR domains consist of approximately 200 residues bearing three conserved motifs, and exhibit sequence similarity to the cytoplasmic domains of the *Drosophila Toll* receptor and the interleukin-1 receptor (IL-1R) (Slack et al., 2000; Jebanathirajaha et al., 2002). This domain activates a downstream signal cascade, leading to HR (Ghelder and Esmenjaud, 2016). Indeed, it has been found that the expression of TIR domains from certain R proteins, such as L6 and RPS4, lead to cell death (Takken and Goverse, 2012). Similarly, CC domains consist of two or more α-helices that wind around each other to form a super-coil (Gruber et al., 2006), and can function as a recognition domain (Rairdan et al., 2008) that like TIR domains, can then mediate a downstream signaling response (Collier and Moffett, 2011; Maekawa et al., 2008).

The identification of candidate genes encoding NB-ARC-LRR proteins that confer resistance to *E. necator* is a crucial step towards a better understanding of the mechanism underlying grapevine-*E. necator* (powdery mildew; PM) interactions and the development of novel sources of resistance to PM. Since grapevine (*Vitis vinifera* L.) is one of the most widely grown and economically important fruit crops in the world and PM caused by the obligate biotrophic fungus *E. necator* (Schw.) is the most destructive disease of grapevine, reducing yield, vine growth and fruit quality (Devi et al., 2013), it is of paramount importance to generate new strategies to mitigate future losses. China is one of the major origins of *Vitis* species, and among the wild species found in this country, a number have been shown to possess high levels of disease resistance to this pathogen (Wang et al., 1995). Hence, Chinese wild *Vitis* species have the potential to provide an incredible resource for furthering our understanding of molecular grapevine-*E. necator* interactions (Gao et al., 2014).

Characterization of several genes containing NB-ARC-LRR domains and the putative molecular mechanisms behind their ability to provide resistance to PM have been described in grapevine previously (Wan et al., 2012). For example, the *Run1* gene from the wild grape species, *Muscadinia rotundifolia*, has been linked to PM resistance, and has been introgressed into *V. vinifera* (Donald et al., 2002; Barker et al., 2005). This gene and its paralog *MrRPV1* were subsequently transformed into a susceptible *V. vinifera* wine grape cultivar, respectively, and in both cases they imparted strong resistance to both PM and downy mildew (Feechan et al., 2013). Likewise, the dominant *REN1* locus from *V. vinifera* 'Kishmish vatkana' has been proposed to provide resistance to PM in this accession (Hoffmann et al., 2008; Coleman et al., 2009).

The Chinese wild grapevine species *Vitis pseudoreticulata* "Baihe-35-1" has been shown to exhibit a relatively high level of resistance to multiple fungi, and particularly *E. necator* (Wang et al., 1995; Yu et al., 2011; 2013a,b). However, as of yet, no studies have been carried out in which NB-ARC-LRR genes related to PM resistance have been identified and functionally characterized in any Chinese wild *Vitis* species. Therefore, to provide a better understanding of the resistance mechanisms involved in defense against *E. necator*, we previously utilized RNA-Seq to investigate the global transcriptional response of *V. pseudoreticulata* "Baihe-35-1" following inoculation with *E. necator* (Weng et al., 2014). Among the genes that were transcriptionally induced by the pathogen, one was predicted to encode a TIR-NB-ARC-LRR domain protein. In this study, we isolated the full-length coding region of this gene, which we designated *VpTNL1*, and carried out a functional characterization via its constitutive heterologous expression in *Arabidopsis thaliana* and *Nicotiana tabacum*. Furthermore, isolation of the *VpTNL1* promoter and subsequent deletion analyses were conducted in an effort to elucidate the mechanism behind its responsiveness to *E. necator* infection and salicylic acid (SA) treatment. Our results indicate that *VpTNL1* contributes to PM disease resistance in Chinese wild *V. pseudoreticulata*, and provide an additional gene target for the future development of grape displaying improved disease resistance.

2. Materials and method

2.1. Plant material and growth conditions

Chinese wild *V. pseudoreticulata* accession "Baihe-35-1" and *V. vinifera* cv. "Red Globe" were maintained in the grape germplasm resources orchard of Northwest A&F University, Yangling, Shaanxi, P. R. China. Grape tissues (young roots, stems, leaves, tendrils, flowers at the fully open stage, and fruits at 33 days post-anthesis) were harvested in the field and immediately frozen in liquid nitrogen. Arabidopsis Col-0 seedlings were grown at 21 °C and 20 °C day and night temperatures, respectively, with 50% relative humidity. Lighting was provided by cool white fluorescent bulbs with an average light intensity of 180 ìmolm^{-2} s^{-1} and a 16/8 h day/night

photoperiod. Tobacco seeds were soaked in water overnight, then surface sterilized with 70% ethyl alcohol for 30 s, immersed in 5% sodium hypochlorite for 10 min, then rinsed in sterile distilled water three times. Seeds were germinated on Murashige and Skoog (1962) (MS) salt medium. Tobacco were grown in a greenhouse with a 16-h day/8-h night photoperiod at 25 °C.

2.2. RNA extraction and first-strand cDNA synthesis

Arabidopsis total RNA was extracted as previously described (Ulker et al., 2007). Total RNA was extracted from grapevine tissues using an improved SDS/phenol method (Zhang et al., 2003) following inoculation with *E. necator* and SA, respectively (Li et al., 2010). Leaves sprayed with sterile distilled water and harvested at the same time points were utilized as untreated controls. First-strand cDNA was synthesized from 500 ng total RNA using the PrimerScript™II 1st Strand cDNA Synthesis kit (TaKaRa Bio Inc., Dalian, China).

2.3. Cloning of VpTNL1 and sequence analysis

The *VpTNL1* cDNA fragment was amplified utilizing gene-specific primers (Supplemental Table 1) and LA Taq DNA polymerase (Takara Bio. Inc.). The resulting PCR product was cloned into the pMD18-T vector (TaKaRa Bio Inc.) and sequenced (Beijing Genomics Institute, Beijing, China) to confirm its identity. The *VpTNL1* nucleotide sequence was analyzed using the BLASTN and BLASTX programs (http://www.ncbi.nlm.nih. gov/BLAST) and its chromosomal location was predicted using the Genoscope Genome Browser (http://www.genoscope.cns.fr/blat-server/cgi-bin/vitis/webBlat). The amino acid sequence and conserved protein domains were deduced using SMART (http://smart.emblheidelberg.de/smart/changemode.pl) and ExPASy (http://au.expasy.org/tools/). The deduced amino acid sequence, including TIR, NB-ARC and LRR domains, was aligned with closely related proteins and a phylogenetic tree was generated using the neighbor joining algorithm and a bootstrap value of 1000 with the ClustalW tool in the MegAlign program (Version 5.07, DNASTAR Inc.).

2.4. Semi-quantitative and quantitative real-time RT-PCR

Semi-quantitative reverse-transcription (RT) PCR reactions were performed using the following profile: initial denaturation at 94 °C for 1 min, followed by 30 cycles of denaturation at 92 °C for 30 s, annealing at 57 °C for 30 s, extension at 72 °C for 30 s, and final extension at 72 °C for 10 min. PCR products were separated on a 1.2% (w/v) agarose gel with ethidium bromide and were imaged under UV light for gene expression analysis. Reactions were repeated three times and all three independent analyses showed the same trends.

For quantitative real-time RT-PCR, reactions were performed using the Bio-Rad IQ5 real-time PCR detection system (Bio-Rad, Hercules, CA, USA). Each reaction was carried out in triplicate with a reaction volume of 20 μl containing 1.0 μl of cDNA as template and SYBR green (TaKaRa Bio Inc.). Reactions were conducted using the following thermal parameters: 30 s at 94 °C, followed by 45 cycles of 5 s at 95 °C, 30 s at 58 °C, and 30 s at 60 °C. For melting curve analysis, 40 cycles at 95 °C for 15 s followed by a constant increase from 60 to 95 °C was utilized. Grape *Actin1* (GenBank Acc. No. AY680701) and *A. thaliana Actin1* (TAIR: AT2G37620) were used as reference genes, respectively. Primer sequences utilized for expression analyses can be found in Supplemental Table 1. All reactions were performed using three biological replicates, each consisting of three leaves harvested from three separate plants, along with three technical replicates. Primer sequences utilized for qRT-PCR are shown in Supplemental Table 1.

2.5. Construction of the heterologous expression vector

To generate the *35S::VpTNL1* heterologous expression construct, the coding sequence of *VpTNL1* was first amplified from pMD18-T-*VpTNL1* using the gene-specific primers VpTNL1-F-G (5' - CCC CGG GGA TGG CTT CTT CTT CAA CCA TTC TCT -3'; *Sma*I site underlined) and VpTNL1-R-G (5' - CCC CGG GGT CAT CCT CAA TAA CCT CGG GTT CAT C -3'; *Sma*I site underlined), cloned into the binary vector, pCAMBIA 2300 (CAMBIA company), downstream of the constitutive CaMV 35S promoter. The resulting plasmid was verified by sequencing and was subsequently introduced into *Agrobacterium tumefaciens* GV3101 via electroporation.

2.6. Arabidopsis transformation

The *35S::VpTNL1* construct was transformed into Arabidopsis using the floral dip method (Clough and Bent, 1998). Transgenic plants were confirmed by both growth on MS media supplemented with 60 mg/L kanamycin and subsequent PCR amplification to verify the presence of the transgene. The three transgenic lines exhibiting the strongest resistance to PM infection (L1, L2 and L3) were grown to the T_3 generation and homozygous plants were utilized throughout the study.

2.7. Tobacco transformation

The *35S::VpTNL1* construct was transformed into tobacco (*Nicotiana tabacum* L. cv. Petit Havana SR1) using the leaf disk transformation method (Horsch et al., 1985) and transgenic plants were selected on regeneration MS agar medium supplemented with 200 mg/L kanamycin, 1 mg/L benzylaminopurine (BA) and 300 mg/L timentin. Following the generation of shoots, plantlets were transferred onto rooting medium (MS agar medium supplemented with 100 mg/L kanamycin, 0.2 mg/L indole-3-butytric acid (IBA) and 300 mg/L timentin). Subsequent extraction of tobacco genomic DNA and PCR amplification was carried out to confirm the presence of the transgenic insertion.

2.8. Construction of VpTNL1 promoter::GUS gene fusion vectors and A. tumefaciens-Mediated transient expression assays

For isolation of the *VpTNL1* upstream region, grapevine genomic DNA was first extracted as described previously (Yu et al., 2013a,b) and subsequent PCR amplification was carried out using primers pVpTNL1-F and pVpTNL1-R (Supplemental Table 1), designed using the Grape Genome Database (12 × ; http://www.genoscope.cns.fr), to amplify a 1498-bp region upstream of the translational start site. The resulting fragment was cloned into pMD18-T and sequenced, and putative regulatory elements were predicted using the PlantCARE program (Lescot et al., 2002) (http://bioinformatics.psb.ugent.be/webtools/plantcare/html/). The resulting *VpTNL1* fragment was then digested with *Pst*I and *Eco*RI, and inserted immediately upstream of the *GUS* gene in the binary vector pC0380::*GUS* (Xu et al., 2010). An empty vector was used as a negative control and *35S::GUS* was used as a positive control (Xu et al., 2010). Two further *pVpTNL1* fragments comprising -900-bp and -240-bp of upstream region were also amplified and cloned into pC0380::*GUS*. In each case, the final constructs were verified via sequencing.

All five constructs, respectively, were introduced into *A. tumefaciens* strain GV3101 via electroporation. *Agrobacterium*-mediated transient expression assays in grapevine leaves were performed as described previously (Santos-Rosa et al., 2008). Briefly, a single *A. tumefaciens* colony transformed with the construct of

interest was grown in liquid Yeast Extract Phosphate (YEP) medium (Smith and Goodman, 1975) supplemented with 100 g/mL kanamycin, 60 g/mL gentamicin and 30 g/mL rifampicin. Bacteria were grown at 28 °C to an OD_{600} of 0.6, then pelleted by centrifugation at 5000 rpm for 10 min, suspended in 5 ml filtration solution (10 mM 2-(N-morpholino) ethanesulfonic acid (MES), pH 5.7, 10 mM $MgCl_2$ and 15 μM acetosyringone) at room temperature for 30 min, and adjusted to an OD_{600} of 0.6. Young *V. vinifera* 'Red Globe' grapevine leaves were used for transformation as previously described (Santos-Rosa et al., 2008; Guan et al., 2011). Following transformation, leaves were rinsed in sterile water and kept in a growth chamber at 23 °C and 70% humidity for 48 h prior to GUS staining.

2.9. Pathogen inoculations and hormone treatments

The *E. necator* pathogen used in this study was *Erysiphe necator* NAFU1 (Gao et al., 2016), the pathogen was maintain on fresh leaves of 'Thompson Seedless', leaves of *V. pseudoreticulata* "Baihe-35-1" were infected by touching the adaxial epidermis of the detached leaves with sporulating colonies from the surface of the source leaves, with each inoculation repeated three times (Wang et al., 1995, 1999; Guan et al., 2011; Gao et al., 2016). A mock inoculation was performed with sterile water. Following inoculation, the leaves were covered with plastic bags for one night to maintain high humidity. Both inoculated and mock-inoculated leaves were harvested at 0, 6, 12, 24, 48, 72 and 96 h post-inoculation (hpi). SA treatments were conducted by spraying leaves with 100 μM SA, and harvested at 0, 0.5, 3, 6, 12 and 24 h post-treatment. Leaves were sprayed with sterile water and harvested at the same time points as a negative control. In both PM inoculation and SA treatment experiments, harvested leaves were immediately flash frozen in liquid nitrogen and stored at -80 °C until use.

The Arabidopsis PM pathogen, *G. cichoracearum*, was maintained on live *pad4* mutant plants at 22 °C with a 16/8 h photoperiod in an incubator for the generation of fresh inoculum. *G. cichoracearum* inoculation was performed on the leaves of 4-week-old wild-type plants, as well as the three transgenic lines (Tang and Innes, 2002). Six biological replicates of each were used for inoculation. Visual scoring of susceptibility or resistance was carried out 8 days post-inoculation (dpi) (Nie et al., 2011). For qRT-PCR experiments, transgenic and wild-type rosette leaves from 4-week-old plants were inoculated and harvested at 0, 12, 24, 36 and 48 hpi.

Pseudomonas syringae pv. tomato (*Pst*) DC3000 was grown overnight in King's B medium with the appropriate antibiotics at 28 °C.Bacterial cells were harvested from liquid culture and washed three times, re-suspended in 10 mM $MgCl_2$ and adjusted to an optical density of $OD_{600} = 0.002$, and finally supplemented with Silwet-77 to a final concentration 0.025%. The bacterial suspension was then injected into the abaxial surface of 6–10 rosette leaves from six wild-type and L1, L2 and L3 transgenic lines, respectively, using a needless 1 ml syringe, and infected plants were grown under 75% humidity.

Erysiphe cichoracearum DC was maintained on *N. tabacum* L. cv. Petit Havana SR1. For *E. cichoracearum* infection, 4–6 leaves from wild-type plants and 12 transgenic tobacco lines were challenged with *E. cichoracearum* DC by spraying them with spore suspension (1.2×10^7 spores/ml water). Inoculated tobacco plants were maintained in a greenhouse with a relative humidity of 80% at 26 °C. Visual scoring of disease severity was carried out 20 dpi (Mu et al., 2014).

2.10. Trypan blue staining

For trypan blue staining, 4–6 Arabidopsis rosette leaves were harvested 12 hpi from six wild-type and L1, L2 and L3 transgenic lines, respectively. Leaves were incubated in trypan blue solution (20 mL ethanol, 10 mL phenol, 10 mL water, 10 mL lactic acid [83%], and 30 mg trypan blue) in a boiling water bath for 2 min, followed by 30 min at room temperature. Stained leaves were then cleared overnight at room temperature and stored in 70% glycerol. Staining was examined with a compound microscope (Koch and Slusarenko, 1990; Frye and Innes, 1998; Wees, 2008). Three independent experiments were performed.

2.11. Peroxide assay

The detection of Arabidopsis O_2^- production was performed using nitroblue tetrazolium (NBT) staining. Rosette leaves from six wild-type and L1, L2 and L3 transgenic lines, respectively, were collected at 24 hpi and stained by vacuum infiltration for 10 min in 2 mM NBT solution in 20 mM phosphate buffer (pH 6.0), followed by incubation room temperature for 1.5 h. Subsequently, leaves were transferred into 95% ethyl alcohol and incubated in an 80 °C water bath for 20 min. Samples were stored in distilled water until photographs were taken (Dunand et al., 2007).

Hydrogen peroxide (H_2O_2) accumulation was measured using a hydrogen peroxide kit, following the manufacturer's instructions (Nanjing Bio Ins., Jiangsu, China). For quantification of dead cells, Arabidopsis rosette leaves were cut into pieces (0.3 mm in diameter) and stained with 0.2% Evans blue (Sigma-Aldrich) for 30 min, then washed several times with distilled water to remove excess stain (Mino et al., 2002; Ahn et al., 2007; Wen et al., 2015). Three independent experiments were performed in each case.

2.12. Callose accumulation

To assess callose accumulation in transgenic Arabidopsis lines, 4–6 rosette leaves from six wild-type and L1, L2 and L3 transgenic lines, respectively, were collected at 3 dpi and incubated in a 1:3 acetic acid: ethanol solution overnight. The samples were then washed with 150 mM K_2HPO_4 several times. Subsequently, the leaves were stained with 150 mM K_2HPO_4 and 0.01% aniline for 1 h, and were then stored in 50% glycerol (Schenk and Schikora, 2015). Callose fluorescence was examined using a fluorescent Zeiss microscope (Jena, Germany) with appropriate filters (Hong et al., 2001).

For quantitative determination of callose, 0.1 g Arabidopsis leaves were immersed in ethanol, which was replaced regularly, for 2 days to remove all traces of chlorophyll. Samples were then centrifuged at 5000×g for 20 min, the supernatant was removed and the pellet was resuspended in 0.4 M DMSO. The resulting solution was boiled for 3 min, cooled at room temperature for 1 h, centrifuged at 5000×g for 20 min and the supernatant was transferred to a new tube. The solution was supplemented with [400 μL 0.1% (w/v) aniline blue, 590 mL 1 M glycine/NaOH (pH 9.5) to 100 μL supernatant. Negative control samples were supplemented with the same solution lacking aniline. Samples were placed in a water bath for 20 min and cooled to room temperature. The fluorescence of the samples was measured with a fluorescence spectrophotometer (F-4600, Hitachi, Tokyo, Japan) with excitation at 393 nm and emission at 479 nm, along with a voltage of 400 V. The level of callose fluorescence was determined by subtracting the fluorescence value of the negative control from those of the experimental samples (Kohler et al., 2000; Wen et al., 2015). Three independent experiments were performed.

2.13. Histochemical and fluorometric GUS assays

Histochemical and fluorometric GUS assays were performed on grapevine transiently transformed with various *pVpTNL1::GUS*

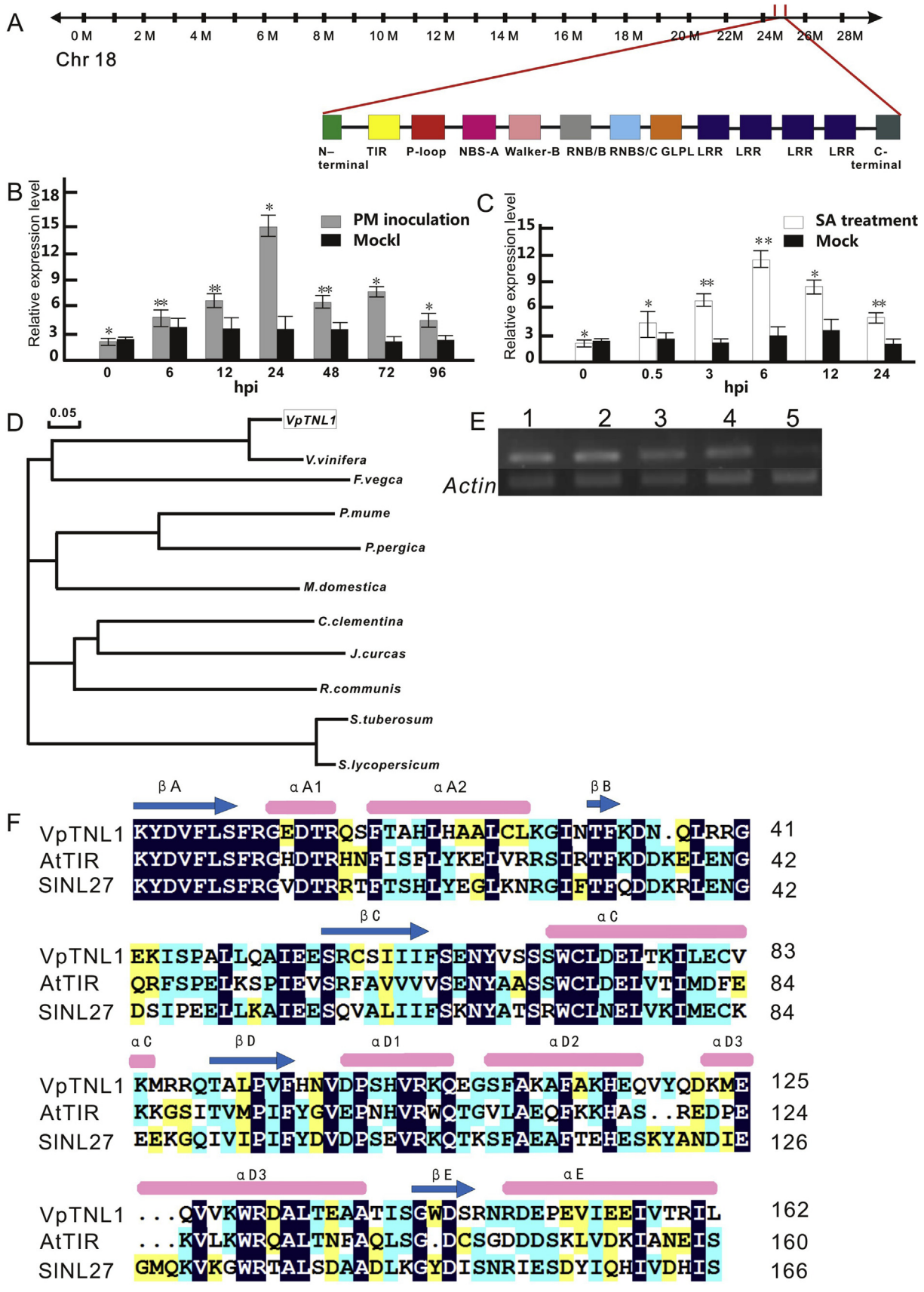
A
0 M
2 M
4 M
6 M
8 M
10 M
12 M
14 M
16 M
18 M
20 M
22M
24M
26M
28M
Chr 18
N–terminal
TIR
P-loop
NBS-A
Walker-B
RNB/B
RNBS/C
GLPL
LRR
LRR
LRR
LRR
C-terminal
B
Relative expression level
PM inoculation
Mockl
hpi
C
Relative expression level
SA treatment
Mock
hpi
D
0.05
VpTNL1
V.vinifera
F.vegca
P.mume
P.pergica
M.domestica
C.clementina
J.curcas
R.communis
S.tuberosum
S.lycopersicum
E
1 2 3 4 5
Actin
F
β A
α A1
α A2
β B
VpTNL1 KYDVFLSFRGEDTRQSFTAHLHAALCLKGINTFKDN.QLRRG 41
AtTIR KYDVFLSFRGHDTRHNFISFLYKELVRRSIRTFKDDKELENG 42
SINL27 KYDVFLSFRGVDTRRTFTSHLYEGLKNRGIFTFQDDKRLENG 42
β C
α C
VpTNL1 EKISPALLQAIEESRCSIIIFSENYVSSSWCLDELTKILECV 83
AtTIR QRFSPELKSPIEVSRFAVVVVSENYAASSWCLDELVTIMDFE 84
SINL27 DSIPEELLKAIEESQVALIIFSKNYATSRWCLNELVKIMECK 84
α C
β D
α D1
α D2
α D3
VpTNL1 KMRRQTALPVFHNVDPSHVRKQEGSFAKAFAKHEQVYQDKME 125
AtTIR KKGSITVMPIFYGVEPNHVRWQTGVLAEQFKKHAS..REDPE 124
SINL27 EEKGQIVIPIFYDVDPSEVRKQTKSFAEAFTEHESKYANDIE 126
α D3
β E
α E
VpTNL1 ...QVVKWRDALTEAATISGWDSRNRDEPEVIEEIVTRIL 162
AtTIR ...KVLKWRQALTNFAQLSG.DCSGDDDSKLVDKIANEIS 160
SINL27 GMQKVKGWRTALSDAADLKGYDISNRIESDYIQHIVDHIS 166

deletion and control constructs and subject to either *E. necator* infection (carried out 24 h after *Agrobacterium* infiltration) or SA treatment (10 mM SA containing 0.05% (v/v) Tween 20, or the same solution lacking SA as a negative control) (Yu et al., 2013a,b). Leaves were collected for GUS assays 24 h following inoculation or treatment. Staining was performed as described previously (Jefferson, 1987), with grapevine leaves incubated in GUS staining solution (Yu et al., 2013a,b) at 37 °C for 24 h. Following staining, leaves were washed in 70% ethanol several times to remove chlorophyll. For quantitative GUS assays, leaf proteins were initially extracted and normalized by dilution with extraction buffer as described previously (Bradford, 1976). GUS activity was expressed as pmol 4-methylumbelliferon (4-MU, Sigma-Aldrich) produced per minute per mg of protein. Three independent experiments were performed in each case.

3. Results

3.1. VpTNL1 expression following powdery mildew inoculation and SA treatment

To identify candidate genes associated with PM resistance, a global transcriptomic analysis of Chinese wild *V. pseudoreticulata* "Baihe-35-1" was carried out previously using RNA-Seq following challenge with *E. necator* (Weng et al., 2014). We observed that the expression of *VpTNL1* was strongly induced after inoculation with *E. necator* NAFU1, which was confirmed in this study via quantitative real-time RT-PCR. Indeed, we observed that *VpTNL1* transcript levels were significantly induced following inoculation with PM at 6, 12 and 24 hpi, with expression levels peaking at 24 hpi and then decreasing subsequently (Fig. 1B). Since SA is known to play an important role in the response of plants to biotrophic pathogens, such as PM, we also sought to determine whether *VpTNL1* was responsive to treatment with this hormone. Analysis of *VpTNL1* expression demonstrated that it was up-regulated significantly following SA treatment, reaching a peak at 6 h post-treatment and then decreasing at 12 and 24 h post-treatment (Fig. 1C). We also evaluated the spatiotemporal expression of *VpTNL1* in leaf, stem, tendril, flower and grape skin tissue. Our results indicated that *VpTNL1* was expressed at high levels in leaves, stems, tendrils and flowers, but only at low levels in grape skin tissue (Fig. 1E).

3.2. Cloning and sequence analysis of VpTNL1

A 3903-bp *VpTNL1* cDNA fragment was isolated from *V. pseudoreticulata* "Baihe-35-1", which was predicted to contain an open reading frame (ORF) of 2622-bp, along with a 1281-bp 3'-untranslated region (GenBank accession number KX649890). BLAST analysis indicated that *VpTNL1* is located on chromosome 18. The deduced encoded protein was found to be 873 amino acids in length (Supplement Fig. 1) with an estimated molecular mass of 99.6 KDa and an isoelectric point (pI) of 8.34. In addition, it is predicted to contain a TIR domain from amino acid residues 23 to 155, an NB-ARC domain from amino acid residues 198 to 474 and four LRR domains from amino acid residues 723 to 736, 771 to 784, 795 to 808 and 842 to 855, respectively (Supplemental Fig. 1). Furthermore, several conserved motifs, such as P-loop, Walker-B, NBS-A, NBS-B, NBS-C and GFPL motifs, were also predicted to be present in the deduced protein.

The full-length VpTNL1 amino acid sequence was also compared to other related putative proteins, and a phylogenetic tree was generated (Fig. 1D). VpTNL1 was found to share 51.5%, 48.0%, 46.4%, 46.0%, 45.9%, 45.0%, 45.0%, 43.8% and 43.2% identity with putative proteins in *Malus domestica* (GenBank accession no. XP008350156), *Fragaria vesca* (GenBank accession no. XP011469998), *Ricinus communis* (GenBank accession no. XP002523481), *Jatropha curcas* (GenBank accession no. XP012076887), *Solanum tuberosum* (GenBank accession no. XP004243783), *Solanum lycopersicum* (GenBank accession no. XP006348979), *Prunus mume* (GenBank accession no. XP008237404), *Prunus persica* (GenBank accession no. XP007227167) and *Citrus reticulata* (GenBank accession no. XP006441860), respectively. Structure-based multiple sequence alignments were also carried out to compare the various conserved domains of the VpTNL1 protein to those of homologous proteins from several other species. The TIR domain of VpTNL1 and AtTIR (GenBank accession no. NP177436) was shown to exhibit 45.1% identity at the amino acid level (Fig. 1F), while the NB-ARC domain of VpTNL1 was found to display 27.1%, 31.4%, and 39.2% identity at the amino acid level with that of AtRPS2 (GenBank accession no. SPQ42484), LpL6 (GenBank accession no. AAA91021) and SiI2C (GenBank accession no. AAB63274), respectively (Fig. 2A). The amino acid identity noted in these domains occurred mainly in the Walker A, Walker B, RNBA-A, RNBS-B, RNBS-C and GLPL conserved motifs. The LRR domains of VpTNL1 was found to share 26.5% identity with a hypothetical *Drosophila melanogaster* protein (GenBank accession no. AF247766), 27.1% identity with a hypothetical *Salmon salar* protein (GenBank accession no. ACN11505), and 39.4% identity with a hypothetical *Danaus plexippus* protein (GenBank accession no. EHJ77461).

3.3. Constitutive expression of VpTNL1 in Arabidopsis and tobacco enhances resistance to powdery mildew

To further study the biological role of *VpTNL1* in defense response, its full-length coding sequence was placed under the control of the constitutive 35S promoter (Fig. 2C) and the resulting cassette was transformed into Arabidopsis Col-0 plants. In total, 49 transgenic independent T_1 lines were obtained. The T_1 progeny exhibited two distinct phenotypes, with 45 of the 49 independent lines displaying a wild-type morphology and the remaining 4 exhibiting an extremely dwarfed stature along with small, yellow leaves (Fig. 3A). Lines with this latter abnormal phenotype died at the seedling stage. Therefore, we chose to use three lines (L1, L2 and L3; T_3 homozygous plants) with a normal phenotype and the strongest resistance response to *G. cichoracearum* for all further experiments. In contrast to wild-type Arabidopsis, the three

Fig. 1. Expression, sequence and phylogenetic analyses of *VpTNL1*. **A** Schematic map of the chromosomal location of *VpTNL1*, along with the major conserved domains and motifs in the deduced VpTNL1 amino acid sequence. **B** Expression of *VpTNL1* in *V. pseudoreticulata* accession "Baihe-35-1" leaves following inoculation with *E. necator*. **C** Expression of *VpTNL1* in *V. pseudoreticulata* accession "Baihe-35-1" leaves following SA treatment. In both B and C, three independent biological replicates were included, with each biological replicate comprising three leaves harvested from three separate plants, and three technical replicates. Bars represent the means ± SE, asterisks indicate statistical significance compared to the negative control (Student's *t*-test, $^{*}P < 0.05$, $^{**}P < 0.01$). **D** Phylogenetic tree generated using the deduced amino acid sequence of VpTNL1 with related sequences from other plants. The amino acids used to generate the phylogenetic tree were: (*Vitis vinifera*, XP010665420), (*Jatropha curcas*, XP012076887), (*Malus domestica,* XP008350156), (*Prunus mume*,XP008237404), (*Solanum tuberosum*, XP004243783), (*Ricinus communis*, XP002523481), (*Solanum tuberosum*, XP006348979) and (*Mandarin orange*, XP006441860). **E** Tissue-specific expression analysis of *VpTNL1* in *V. pseudoreticulata* accession "Baihe-35-1" leaves, stems, tendrils, flowers, and grape skin tissue using semi-quantitative RT-PCR. Lanes 1, 2, 3, 4 and 5 indicate leaves, stems, tendrils and grape skin tissue, respectively. **F** Amino acid alignment of the VpTNL1 TIR domain with *A. thaliana* and *S. tuberosum* TIR protein domains (GenBank accession nos. NP177436 and XP006359566, respectively), along with prediction of the secondary structure of the VpTNL1 TIR domain.

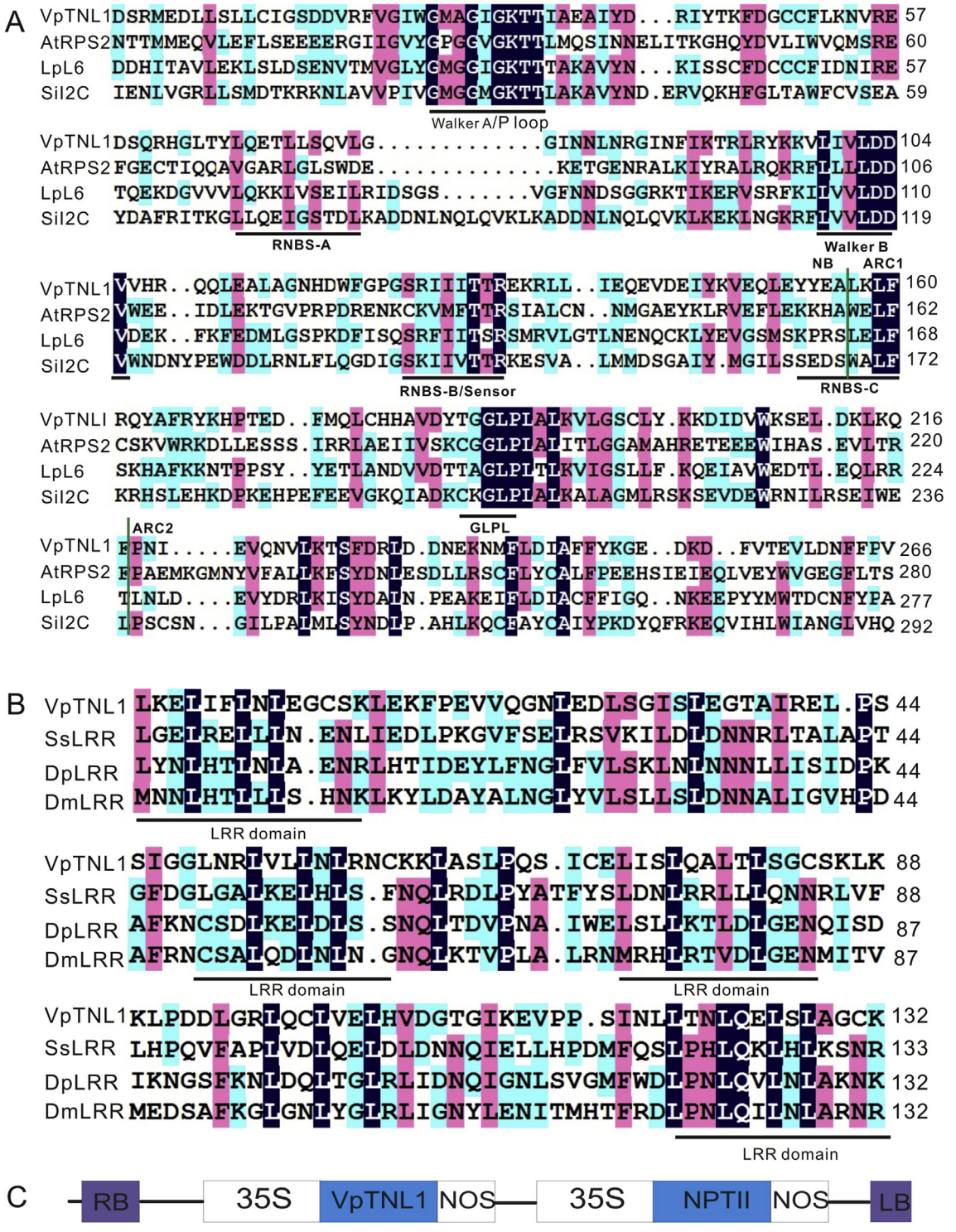

Fig. 2. Alignment of NB-ARC and LRR domains and *35S::VpTNL1* plant transformation construct. **A** Multiple sequence alignment of the VpTNL1 NB-ARC domain with those of closely related proteins, including *A. thaliana* RPS2 (GenBank accession no. SPQ42484), *Linum ustitatissimum* L6 (GenBank accession no. AAA91021), and *Solanum lycopersicon* I2C (GenBank accession no. AAB63274). **B** Multiple sequence alignment of the VpTNL1 LRR domain with those of closely related proteins, including *Drosophila melanogaster* (GenBank accession no. AF247766), *Salmon salar* (GenBank accession no. ACN11505) and *Danaus plexippus* (GenBank accession no. EHJ77461). **C** Schematic diagram (not to scale) of the *35S::VpTNL1* vectors for transformation of Arabidopsis and tobacco.

transgenic lines displayed very few disease symptoms 8 dpi with *G. cichoracearum* (Fig. 3B and C). Furthermore, the expression levels of pathogenesis-related protein 1 (*PR1*) were evaluated via qRT-PCR at 0, 12, 24, 36 and 48 hpi with *G. cichoracearum* to test whether enhanced resistance to this pathogen was related the expression of such a defense-related gene. Our results demonstrated that *PR1* transcript levels were significantly higher (3–4-fold) than wild-type by 12 hpi, and remained elevated at all subsequent time points tested (Fig. 3D).

Furthermore, the majority of transgenic tobacco (*N. tabacum* L.

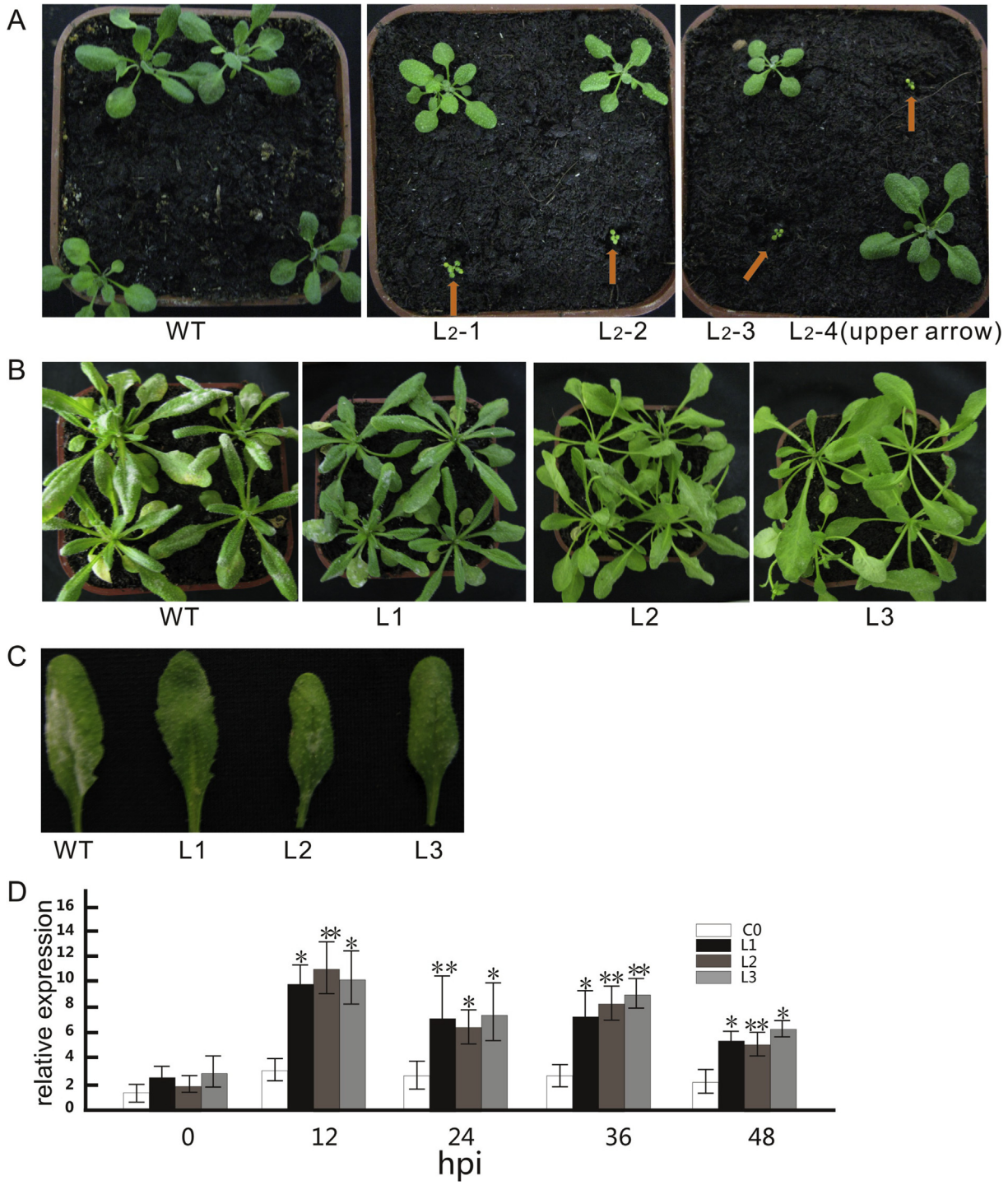

Fig. 3. Morphology of transgenic Arabidopsis and wild-type plants, and response to *G. cichoracearum* inoculation. **A** T_1 transgenic Arabidopsis plants displayed either a normal phenotype or a dwarfed stature (indicated by an arrow). **B** Wild-type and transgenic lines (L1, L2 and L3) 8 days post-inoculation (dpi) with *G. cichoracearum*. Disease symptoms consisted of white powdery lesions on plants, with wild-type plants displaying more severe symptoms than transgenic lines. **C** Disease symptoms on individual leaves 8 dpi. **D** Relative expression levels of *PR1* in wild-type and transgenic lines 0, 12, 24, 36, and 48 h post-inoculation (hpi) with *G. cichoracearum*. The experiment encompassed three biological replicates, each consisting of six rosette leaves from three separate plants, and three technical replicates. Bars represent means ± SE, asterisks indicate statistical significance compared to wild type (Student's *t*-test, *P < 0.05, **P < 0.01).

cv. Petit Havana) stably transformed with the 35S-VpTNL1 construct (Fig. 4A) died at the seedling stage (data not shown), with 13 viable transgenic tobacco lines obtained. The resulting transgenic plants displayed two phenotypes, with 12 of 13 lines displaying a wild-type phenotype and the remaining transgenic line displaying a stunted phenotype that did not produce flowers or seeds (Fig. 4B). The phenotypically normal transgenic tobacco lines were selected for *E. cichoracearum* DC challenge (Fig. 4B C), whereby transgenic plants showed fewer symptoms following inoculation than wild-type tobacco (Fig. 4E). Indeed, statistical

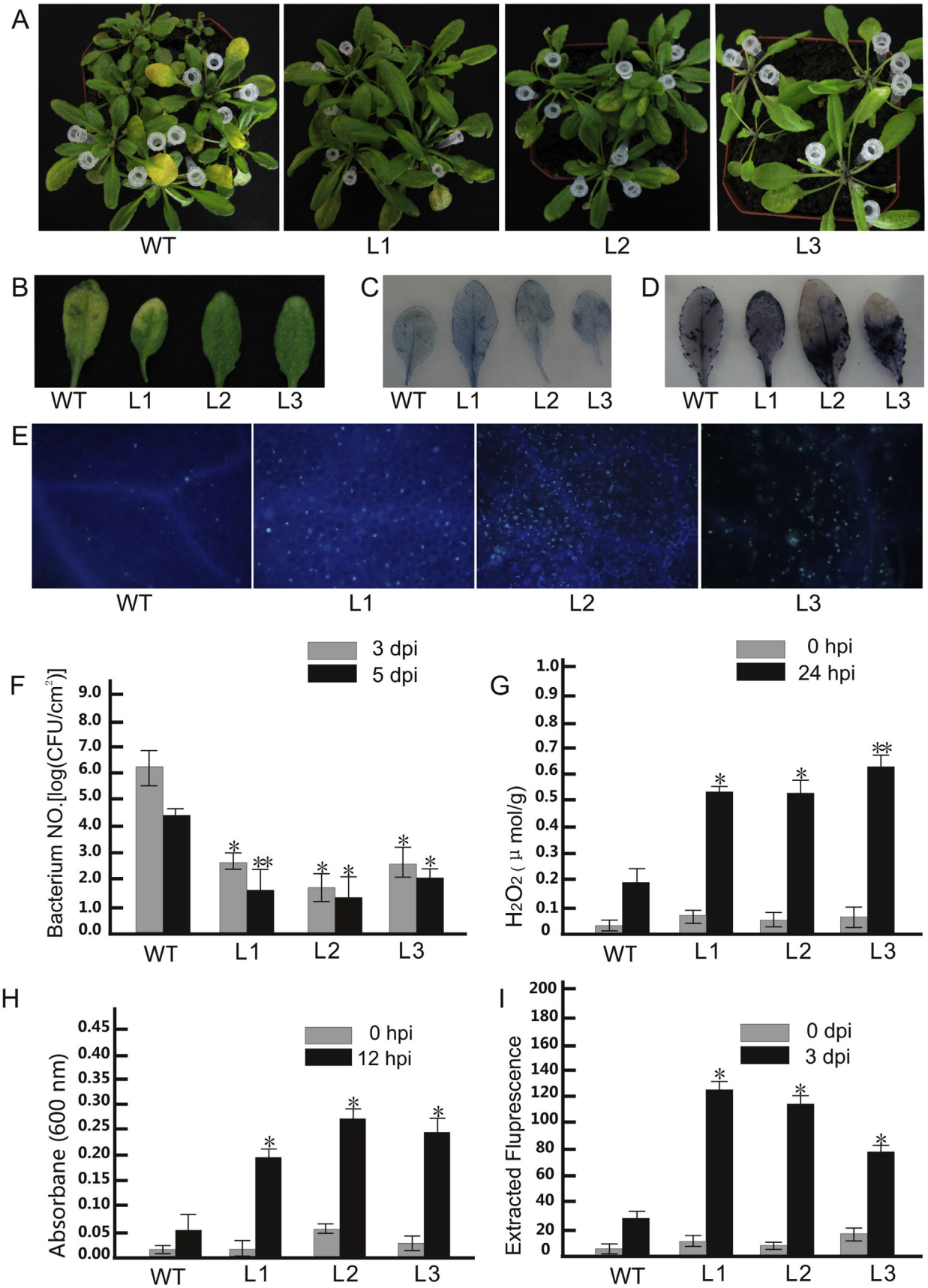

Fig. 4. Constitutive expression of *VpTNL1* in tobacco increases resistance to *E. cichoracearum* DC. **A** Adventitious bud formation from wild-type and transgenic tobacco calli. **B** Phenotypes of wild-type and transgenic tobacco. Lines L1 and L2 displayed a normal phenotype, while L3 displayed a sterile phenotype. **C** Microscopic examination of *E. cichoracearum* DC spores prior to inoculation. **D** Disease symptoms on wild-type and transgenic tobacco leaves at 21 dpi with *E. cichoracearum* DC.

analyses indicated that the PM disease index of transgenic tobacco was significantly lower than wild-type controls.

3.4. Constitutive expression of VpTNL1 in aArabidopsis enhances resistance to Pst DC3000

Interestingly, a PLN03210 domain was predicted within the VpTNL1 amino acid sequence, which has been reported to be correlated with resistance to *P. syringae* pv. glycinea race 6 (Kim et al., 2009). We therefore hypothesized that *VpTNL1* could also play a role in providing resistance to bacterial infection. To test this hypothesis, transgenic (L1, L2 and L3) and wild-type plants were inoculated with the bacterial pathogen, *Pst* DC3000, and disease symptoms were assessed. In wild-type plants, severe symptoms were noted 3 dpi, with yellowing leaves and spreading macerations (Fig. 5A and B). In the three transgenic lines tested, less severe symptoms were observed 3 dpi than those present in wild type (Fig. 5A and B).

To determine whether this enhancement in resistance resulted from the inhibition of bacterial growth, a colony counting assay was utilized to assess growth of *Pst* DC3000 in infected leaves. Bacterial number was significantly reduced in transgenic lines (L1, L2 and L3) compared to wild-type plants (Fig. 5F) following infection. To observe the effect of heterologous *VpTNL1* expression on cell death, infected leaves were stained with trypan blue 12 hpi, with large clusters of dead cells visible in transgenic leaves and very few dead cells apparent in wild-type plants (Fig. 5C). To further quantify cell death following infection, infected leaves were stained with Evans blue and fluorescence was analyzed. Our results demonstrated that transgenic lines exhibited a 7–10-fold enhancement in the level of cell death compared to wild-type plants (Fig. 4H). Nitroblue tetrazolium (NBT) staining was performed in transgenic and wild-type plants to detect superoxide anion accumulation, with results revealing a substantial and significant increase in the accumulation of O_2^- in transgenic plants compared to wild-type plants following infection (Fig. 5D). Similarly, quantitative detection of H_2O_2 showed that levels of H_2O_2 in transgenic plants were 2–3 fold higher than wild-type plants following challenge with this bacterial pathogen (Fig. 5G). To examine callose deposition following pathogen inoculation, infected leaves were stained with aniline blue. We found that the level of callose deposition in transgenic plants was significantly increased compared to wild-type plants (Fig. 5E), with

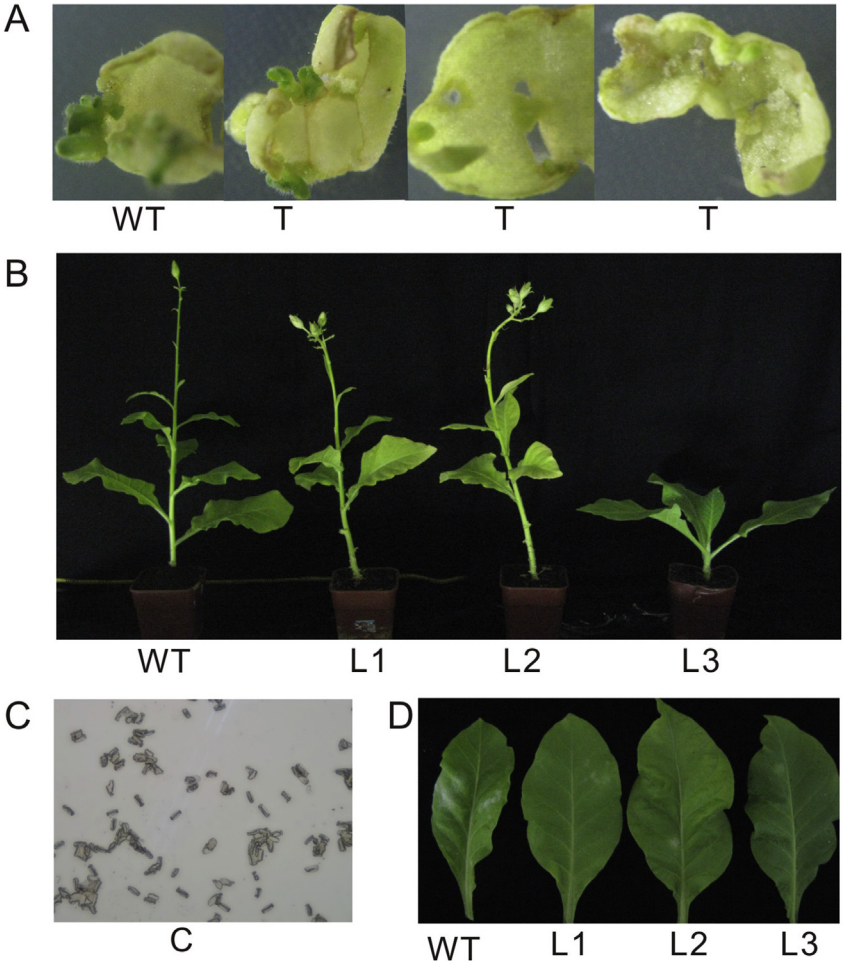

Fig. 5. Constitutive heterologous expression of *VpTNL1* in Arabidopsis enhances disease resistance to *Pst* DC3000. **A** Disease symptoms caused by *Pst* DC3000 in wild-type and transgenic lines (L1, L2 and L3). Injected leaves were marked with white pipette tips and pictures were taken 3 d post-inoculation (dpi). **B** Disease symptoms on individual leaves 3 dpi with *Pst* DC3000. **C** Trypan blue staining of leaves from wild-type and transgenic lines inoculated with *Pst* DC3000. **D** Nitro blue terazolium (NBT) staining of inoculated leaves from wild-type and transgenic plants. **E** Microscopic examination of callose deposition following inoculation of leaves from wild-type and transgenic lines. **F** Bacterial growth was measured on the leaves of wild-type and transgenic lines at 3 and 5 dpi with *Pst DC3000*. **G** H_2O_2 concentration in the leaves of wild-type and transgenic lines at 0 and 24 h post-inoculation (hpi) with *Pst DC3000*. **H** Quantification of cell death in the leaves of wild-type and transgenic lines at 12 hpi. **I** Quantification of callose accumulation in the leaves of wild-type and transgenic lines at 3 dpi. Experiments encompassed three biological replicates, with each consisting of six rosette leaves from three separate plants, and three technical replicates. Bars represent means ± SE, asterisks indicate statistical significance compared to wild type (Student's *t*-test, $^*P < 0.05$, $^{**}P < 0.01$).

further quantification demonstrating that transgenic plants accumulated 4–6-fold more callose than wild-type plants following infection (Fig. 5I).

3.5. Isolation and analysis of the VpTNL1 promoter sequence

A 1,498-bp upstream sequence of *VpTNL1* was isolated from wild Chinese *V. pseudoreticulata* "Baihe-35-1" genomic DNA (Supplement Fig. 2) (GenBank accession number KX649891), and putative regulatory elements within it were predicted (Fig. 6A). The resulting *cis*-elements could be classified into three groups, with the first including basal transcriptional regulatory elements, such as 32 TATA boxes and 25 CAAT box elements. The second group included *cis*-elements involved in abiotic and hormonal response, such as 8 SA-responsive TCA elements, 4 defense and stress-responsive TC-rich elements (Supplement Fig. 2), 1 auxin-responsive AuxRR-element, 3 heat-stress HSE elements and 3 drought-induced MBS elements. The third group included light-responsive elements, such as 1 L-box, 1 ATCT-motif, 1 Box4, 1 CATT-motif, 1 MRE motif and 3 SP1 elements. In addition, several other *cis*-elements were also predicted within this upstream region, such as ARE, G4N4-motif, HD-Zip, and HD-Zip2 elements. Based on the presence of predicted regulatory elements involved in response to biotic and abiotic stress, these results suggest that the *VpTNL1* promoter plays a role in its involvement in biotic and abiotic stress-response.

3.6. Activation of the VpTNL1 promoter by PM infection and SA treatment

To test the transcriptional responsiveness of the *VpTNL1* promoter, the 1498-bp promoter fragment was fused upstream of the *GUS* reporter gene (Fig. 6B), and GUS activity was examined following *Agrobacterium*-mediated transient expression assays in grapevine leaves. The *35S::GUS* cassette was utilized as a positive control and *pC0380::GUS* (Xu et al., 2010), which includes a promoterless *GUS* cassette, was used as a negative control. GUS activity was examined using both histochemical staining and fluorometric assays following inoculation with *E. necator* NAFU1 or treatment with SA. Leaves transformed with the *35S::GUS* construct exhibited strong GUS activity, while *pVpTNL1::GUS*-transformed grapevine leaves displayed lower levels of GUS activity. No GUS activity was detected in mock and negative control transformed leaves (Fig. 6C). Following inoculation with *E. necator* NAFU1 or SA treatment, transformed leaves displayed similar levels of GUS staining as mock-inoculated control leaves (Fig. 7B). However, when GUS activity was quantified fluorometrically, our results indicated that GUS activities were increased 1.43- and 1.71-fold in transformed

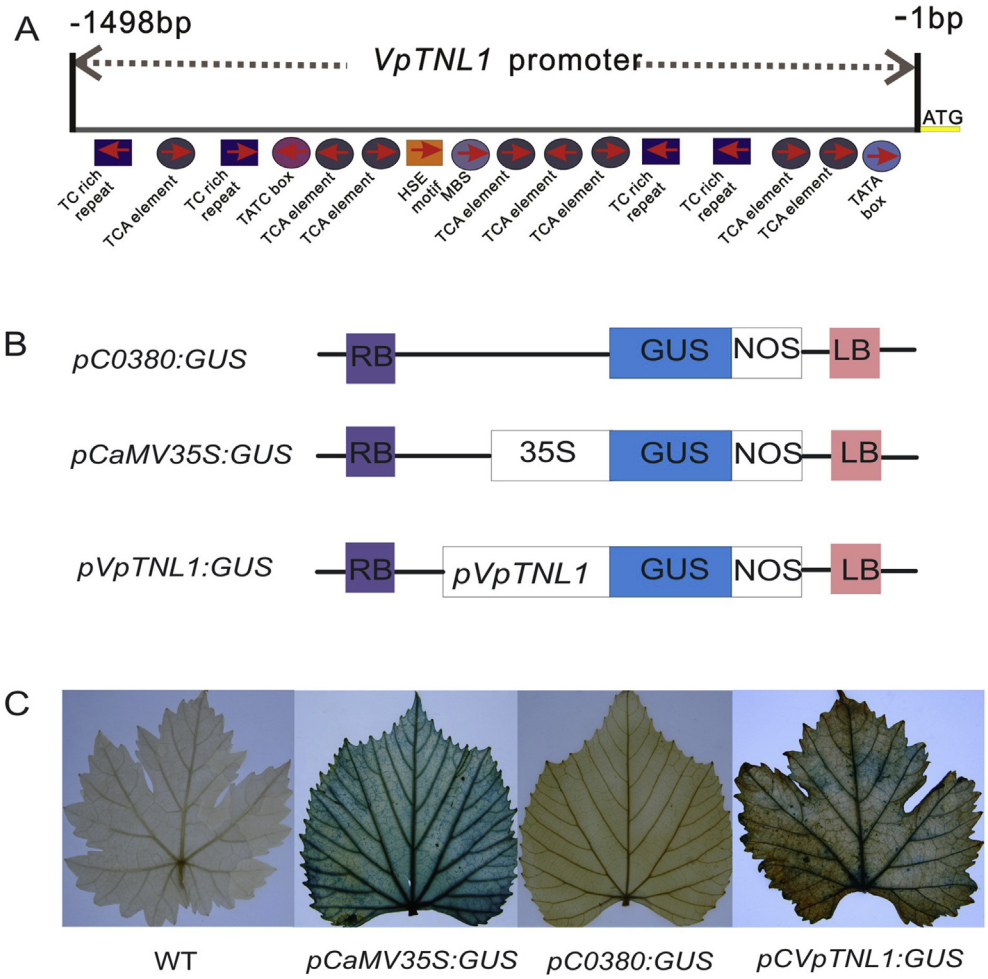

Fig. 6. Major predicted *cis*-elements in the *VpTNL1* promoter sequence and *pVpTNL1::GUS* fusion experiments. **A** Schematic diagram of the major predicted *cis*-acting elements in the 1498-bp upstream region of *VpTNL1*. **B** Schematic diagrams (not to scale) of the *pVpTNL1::GUS* vector for *Agrobacterium*-mediated transient expression in grapevine leaves, along with pC0380::*GUS* (negative control) and *35S::GUS* (positive control). **C** GUS histochemical assay of *V. vinifera* 'Red Globe' following *Agrobacterium*-mediated transient expression of the GUS fusion vectors.

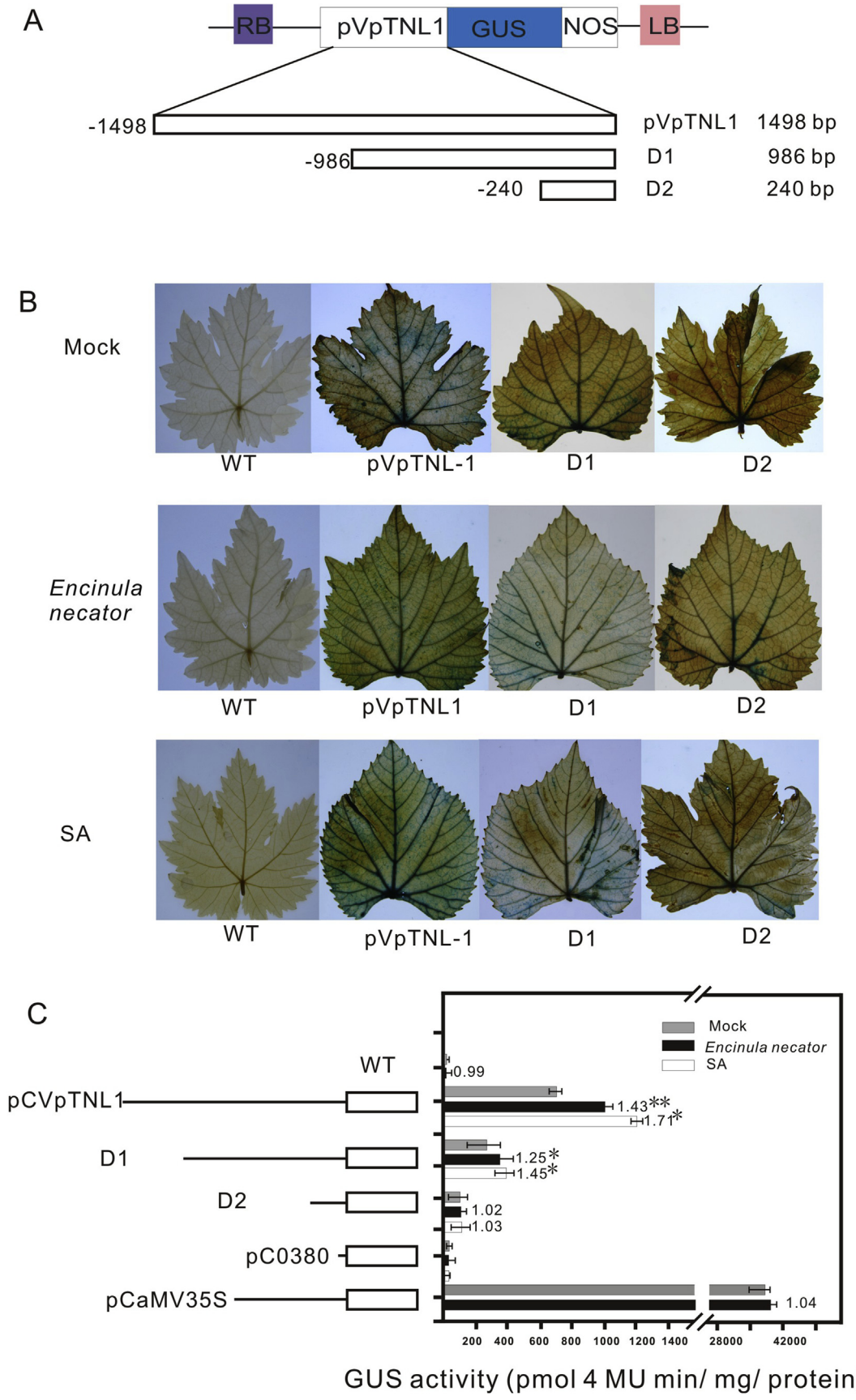

Fig. 7. *VpTNL1*::*GUS* deletion constructs and GUS analysis of grapevine leaves following inoculation with *E. necator* NAFU1 and SA treatment. **A** Schematic diagram (not to scale) of *pVpTNL1* promoter 5′ deletions fused to GUS. **B** GUS histochemical assay of grapevine leaves transiently expressing each of the deletion constructs following mock-treatment, inoculation with *E. necator* NAFU1, and SA treatment. **C** Quantitative determination of GUS activity in grapevine leaves transiently expressing each of the deletion constructs. GUS activity was measured 24 h after inoculation with *E. necator* and SA treatment. The mean GUS activity (±SD) was calculated from three independent experiments ($n = 3$). Numbers on left indicate the fold induction of GUS activity, and the significant differences were assessed using one-side paired *t*-test (**P < 0.01, *P < 0.05).

leaves following inoculation with *E. necator* NAFU1 and SA treatment, respectively, over mock-treated controls (Fig. 7C). To narrow down the location of possible pathogen-responsive and SA-responsive *cis*-elements, we also generated two 5′ truncated *pVpTNL1* fragments (-900-bp and -240-bp) and inserted them upstream of *GUS* (Fig. 7A). GUS activity was found to be induced 1.25- and 1.45-fold following inoculation with *E. necator* NAFU1 and SA treatment than mock treatment in leaves transformed with the -900-bp cassette, respectively, while no significant difference was found in GUS activity between treated and untreated leaves transformed with the -240-bp cassette (Fig. 7C).

4. Discussion

We previously analyzed the leaf transcriptome of wild Chinese *V. pseudoreticulata* "Baihe-35-1" following challenge with the causal agent of PM, *E. necator*, and identified a gene that is predicted to encode a TIR-NA-ARC-LRR domain that was up-regulated substantially following inoculation (Weng et al., 2014). In the present study, we isolated the ORF sequence of this gene, which we have termed *VpTNL1*, and constitutively expressed it in Arabidopsis and tobacco. These resulting transgenic lines were then assessed for their response to fungal and bacterial infection. In addition, we also isolated the upstream promoter region of this gene and generated a *VpTNL1* promoter:*GUS* fusion, along with two further 5' promoter deletion cassettes, in an attempt to elucidate the region involved in transcriptional response to pathogen attack.

The expression of NB-ARC-LRR genes has frequently been found to be up-regulated in plants infected by pathogens (Wan et al., 2012; Arya et al., 2014; Rodamilans et al., 2014; Zhang et al., 2016), and as such, they have been proposed to be involved in the monitoring of pathogenic microbes (Mukhtar et al., 2011; Zhang et al., 2016) or the activation of a downstream defense signaling pathway (Gassmann et al., 1999). In line with this, the *VpTNL1* gene examined in this study was found to be expressed at significantly higher levels in *V. pseudoreticulata* "Baihe-35-1" leaves following challenge with the causal agent of PM, *E. necator* (Fig. 1B). In addition, we also found that the exogenous application of SA to grapevine leaves resulted in up-regulation of *VpTNL1* (Fig. 1C), which corresponds well with previous reports in which application of this phytohormone resulted in a similar phenomenon in Arabidopsis (Nandety et al., 2013; Mohr et al., 2010). Given the fact that SA plays a central role in the activation of both local defense reactions and the induction of systemic resistance, our results suggest that the function of *VpTNL1* in disease resistance may be achieved, at least in part, via the SA signaling pathway.

Several reports have indicated that the constitutive overexpression of R genes can be harmful to plants. Indeed, it has often been associated with a dwarfed stature, and in some cases lethality (Stokes et al., 2002; Shirano et al., 2002; Frost et al., 2004; Li et al., 2007; Nandety et al., 2013), which has been proposed to be the result of a fitness cost underlying the necessity for tight regulation of R genes (Heil and Baldwin, 2002; Li et al., 2007). Consistent with these previous results, we found that approximately 8% of our independent transgenic T_1 Arabidopsis lines displayed stunted growth, small yellow leaves, and eventual death. Similarly, the majority of our transgenic tobacco lines died at the seedling stage. These findings suggest that expression of *VpTNL1* from the 35S promoter in these lines caused constitutive defense activation or toxicity in plants, although the exact mechanism by which this occurs remains to be determined.

In addition to the abnormal phenotypes sometimes observed in plants transgenically expressing R genes, various studies have also found that overexpression of these genes yields broad spectrum enhancement of resistance to pathogens as a result of up-regulation of *PR1* expression (Li et al., 2007). For example, this effect has been noted with *Prf* and *Pto* overexpression in tomato, respectively (Oldroyd and Staskawicz, 1998; Tang et al., 1999), as well as *Cf-9* overexpression in tobacco (Wulff et al., 2004). We also found a broad spectrum enhancement in disease resistance in our phenotypically normal *VpTNL1* transgenic Arabidopsis lines compared to wild type, with improved resistance to both the fungal species, *G. cichoracearum* (the causal agent of PM; Fig. 3), and the bacterial *Pst* DC3000 (Fig. 4). Similarly, *VpTNL1* transgenic tobacco lines were found to exhibit superior resistance to *E. cichoracearum* (the causal agent of PM; Fig. 5). As has been found previously, this enhancement in disease resistance appears to result, at least in part, from up-regulation of *PR1* expression, since *PR1* transcript levels were found to be 3–4-fold higher in our *VpTNL1* transgenic Arabidopsis lines following challenge with *G. cichoracearum* than in wild-type plants (Fig. 3D).

Reactive oxygen species play an important role in plant defense against various pathogens (Mittler et al., 2004; Torres et al., 2006), with hydrogen peroxide (H_2O_2) and superoxide anion (O_2^-) being the two main forms. In this study, *VpTNL1* transgenic Arabidopsis lines displayed more rapid and higher levels of ROS accumulation (H_2O_2 and O_2^-) than wild-type plants following inoculation with *Pst* DC3000 (Fig. 4 D, G). It is conceivable that this type of rapid ROS accumulation has the potential to be directly toxic to the pathogen (Lamb and Dixon, 1997), and could also lead to an enhanced HR that results in host cell death, thus preventing pathogen spread (Heath, 2000; Torres et al., 2006; http://www.ncbi.nlm.nih.gov/pmc/articles/PMC2815885/Gechev et al., 2006). Indeed, high concentrations of ROS are known to lead to oxidative stress, causing HR-like cell death in plants (Kovtun et al., 2000; Zhang et al., 2012), and over-expression of various R genes in plants have been found to induce HR-like cell death previously (Weaver et al., 2006; Oldroyd and Staskawicz, 1998; Zhang et al., 2004). In the present study, constitutive expression of *VpTNL1* in Arabidopsis was also shown to increase HR-like cell death following inoculation with *Pst* DC3000 (Fig. 4 C, H), which suggests that the oxidative burst following infection likely triggers HR-like cell death, enhancing resistance to the pathogen. While these results are intriguing, it is possible that the oxidative burst observed in our transgenic lines could also trigger additional alterations that promote disease resistance, such as the activation of downstream defense gene expression (http://www.ncbi.nlm.nih.gov/pmc/articles/PMC2815885/Dat et al., 2000; http://www.ncbi.nlm.nih.gov/pmc/articles/PMC2815885/Grant and Loake, 2000).

Along with ROS, the production of callose is also known to play a role in plant disease defense, providing a physical barrier to slow pathogen invasion and contributing to plant innate immunity (Luna et al., 2011; Jones and Dangl, 2006). Indeed, it has been proposed that *pmr4* Arabidopsis mutants, which are resistant to PM, are able to resist penetration of the fungus via the deposition of callose (Jacobs et al., 2003; Ellinger et al., 2013). Similarly, overexpression of *Pto* in tomato causes an increase in callose deposition and a significant restriction of pathogen growth (Tang et al., 1999). Likewise, our *VpTNL1* transgenic Arabidopsis lines were also found to exhibit an augmentation in the deposition of callose compared to wild-type plants following inoculation with *Pst* DC3000, which likely contributed to enhanced resistance to this pathogen (Fig. 4 E, I). Interestingly, it has been proposed that callose biosynthesis is induced by the production of ROS (Luna et al., 2011). Since ROS were found to accumulate to higher levels in our transgenic lines than in wild-type plants, it is tempting to speculate that this may be a factor in the increased production of callose in these lines. However, further study will be needed to determine the exact factors involved in callose accumulation in *VpTNL1* transgenic lines in response to pathogen challenge.

The promoter sequence of *VpTNL1* was predicted to contain four TC-rich repeats (5′-ATTCTCTAAC-3′), which are believed to be involved in defense and stress response (Diaz-De-Leon et al., 1993), and eight TCA elements (5′-CAGAAAAGGA-3′), which have been proposed to play a role in SA-mediated response (Goldsbrough et al., 1993). It is therefore feasible that these motifs may be involved in the transcriptional response of *VpTNL1* to *E. necator* and SA treatment, respectively (Fig. 7 B). We generated two further 5′ promoter deletion constructs to test this hypothesis, with the first (-900-bp) containing two TC-rich repeats and eight TCA elements, and the second (-240-bp) bearing no TC-rich repeats or TCA elements. The GUS activity in grapevine leaves containing the -900-bp deletion construct increased 1.25- and 1.45-fold following inoculation with PM and SA treatment, respectively, compared to mock treatment. Conversely, grapevine leaves containing the -240-bp deletion construct displayed no significant change in GUS activity following inoculation with *E. necator* or SA treatment compared to mock-treated controls, which corroborates the proposal that the TC-rich and TCA elements play a role in its transcriptional response.

In conclusion, our results suggest that *VpTNL1* functions to confer at least some level of resistance to both fungal and bacterial pathogens in plants, and that this ability is mediated, at least in part, via the up-regulation of *PR1*. Furthermore, it appears that promoter elements located between -240 and -900-bp upstream of the translational start codon (possibly TC-rich repeats and TCA elements) are involved in the transcriptional up-regulation of this gene seen in response to PM infection and SA treatment, respectively. Future investigations of a possible interaction between VpTNL1 and an *E. necator* AVR (effector) protein, along with other possible proteins that elicit downstream defense responses, will provide further understanding of the molecular mechanisms behind the high level of disease resistance observed in Chinese wild *V. pseudoreticulata*.

Contributions

XW, ZL and ZW designed the study. ZW and LY performed the experiments. ZW, LY, HM and ZL analyzed the results, XW and ZL provided overall guidance throughout the study, ZW, SS and XW wrote the manuscript. All authors read and approved the final manuscript.

Acknowledgements

This work was supported by the National Natural Science Foundation of China (31572110 and 31501740) and the Program for Innovative Research Team of Grape Germplasm Resources and Breeding (2013KCT-25).

Appendix A. Supplementary data

Supplementary data related to this article can be found at http://dx.doi.org/10.1016/j.plaphy.2017.01.017.

References

Ahn, L.P., Kim, S., Lee, Y.H., Suh, S.C., 2007. Vitamin B1-induced priming is dependent on hydrogen peroxide and the *NPRl* gene in *Arabidopsis*. Plant Physiol. 143, 838–848.

Ahuja, I., Kissen, R., Bones, A.M., 2012. Phytoalexins in defense against pathogens. Trends Plant Sci. 17, 73–90.

Arya, P., Kumar, G., Acharya, V., Singh, A.K., 2014. Genome-wide identification and expression analysis of NBS-encoding genes in *Malus* × *domestica* and expansion of NBS genes family in Rosaceae. PLoS One 9, e107987.

Barker, C.L., Donald, T., Pauquet, J., Ratnaparkhe, M.B., Bouquet, A., Adam-Blondon, A.F., Thomas, M.R., Dry, I.B., 2005. Genetic and physical mapping of the grapevine powdery mildew resistance gene, *Run1*, using a bacterial artificial chromosome library. Theor. Appl. Genet. 111, 370–377.

Berger, S., Sinha, A.K., Roitsch, T., 2007. Plant physiology meets phytopathology: plant primary metabolism and plant-pathogen interactions. J. Exp. Bot. 58, 4019–4026.

Boller, T., Felix, G., 2009. A renaissance of elicitors: perception of microbe associated molecular patterns and danger signals by pattern-recognition receptors. Annu. Rev. Plant Biol. 60, 379–406.

Bradford, M.A., 1976. Rapid and sensitive method for the quantitation of microgram quantities of protein utilizing the principle of proteindyebinding. Anal. Biochem 72, 248–254.

Clough, S.J., Bent, A.F., 1998. Floral dip: a simplified method for *Agrobacterium*-mediated transformation of *Arabidopsis thaliana*. Plant J. 16, 735–743.

Coleman, C., Copetti, D., Cipriani, G., Hoffmann, S., Kozma, P., Kovács, L., Morgante, M., Testolin, R. Di, Gaspero, G., 2009. The powdery mildew resistance gene *REN1* co-segregates with an NBS-LRR gene cluster in two Central Asian grapevines. BMC Genet. 10, 89.

Collier, S.M., Moffett, P., 2011. NB-LRRs work a 'bait and switch' on pathogens. Trends Plant Sci. 14 (10), 521–529.

Dangl, J.L., Jones, J.D.G., 2001. Plant pathogens and integrated defense responses to infection. Nature 411 (6839), 826–833.

Dat, J., Vandenabeele, S., Vranova, E., Van Montagu, M., Inze, D., Van Breusegem, F., 2000. Dual action of the active oxygen species during plant stress responses. Cell Mol. Life Sci. 57, 779–795.

Devi, P.A., Vinothini, K., Prakasam, V., 2013. Effect of azoxystrobin 8.3%w/w + mancozeb 68.75% on powdery and downy mildew pathogens under in vitro condition. Agric. Veterinary Sci. 6 (4), 50–55.

Diaz-De-Leon, F., Klotz, K.L., Lagrimini, M., 1993. Nucleotide sequence of the tobacco (*Nicotiana tabacum*) anionic peroxides gene. Plant Physiol. 101, 1117–1118.

Donald, F.M., Pellerone, F., Adam-Blondon, A.F., Bouquet, A., Thomas, M.R., Dry, I.B., 2002. Identification of resistance gene analogs linked to a powdery mildew resistance locus in grapevine. Theor. Appl. Genet. 104, 610–618.

Dunand, C., Crèvecoeur, M., Penel, C., 2007. Distribution of superoxide and hydrogen peroxide in *Arabidopsis* root and their influence on root development: possible interaction with peroxidases. New Phytol. 174, 332–341.

Ellinger, D., Naumann, M., Falter, C., Zwikowics, C., Jamrow, T., Manisseri, C., et al., 2013. Elevated early callose deposition results in complete penetration resistance to powdery mildew in *Arabidopsis*. Plant Physiol. 161, 1433–1444.

Feechan, A., Anderson, C., Torregrosa, L., Jermakow, A., Mestre, P., Wiedemann, M.S., et al., 2013. Genetic dissection of a TIR-NB-LRR locus from the wild North American grapevine species *Muscadinia rotundifolia* identifies paralogous genes conferring resistance to major fungal and oomycete pathogens in cultivated grapevine. Plant J. 76, 661–674.

Fenyker, S., Townsend, P.D., Dixon, C.H., Spies, G.B., Campillo, Alba de SE., et al., 2015. The Potato nucleotide-binding leucine-rich repeat (NLR) immune receptor *Rx1* is a Pathogen-dependent DNA-deforming protein. Biol. Chem. 290 (41), 24945–24960.

Frost, D., Way, H., Howles, P., Luck, J., Manners, J., Hardham, A., Finnegan, J., Ellis, J., 2004. Tobacco transgenic for the Flax Rust resistance Gene *L* expresses allele-specific activation of defense responses. Mol. Plant Microbe Interact. 17 (2), 224–232.

Frye, C.A., Innes, W., 1998. An *Arabidopsis* mutant with enhanced resistance to powdery mildew. Plant Cell 10, 947–956.

Gao, F., Dai, R., Pike, S.M., Qiu, Q.P., Gassmann, W., 2014. Functions of EDS1-like and PAD4genes in grapevine defenses against powdery mildew. Plant Mol. Biol. 86, 381–393.

Gao, Y.U., Han, Y.T., Zhao, F.L., Li, Y.J., Cheng, Y., Ding, Q., Wang, Y.J., Wen, Y.Q., 2016. Identification and utilization of a new *Erysiphe necator* isolate NAFU1 to quickly evaluate powdery mildew resistance in wild Chinese grapevine species using detached leaves. Plant Physiol. Bioch 98, 12–24.

Gassmann, W., Hinsch, M.E., Staskawicz, B.J., 1999. The *Arabidopsis* RPS4 bacterial-resistance gene is a member of the TIR-NBS-LRR family of disease resistance genes. Plant J. 20, 265–277.

Gechev, T.S., Breusegem, F.V., Stone, J.M., Denev, I., Loloi, C., 2006. Reactive oxygen species as signals that modulate plant stress responses and programmed cell death. Bioessays 28, 1091–1101.

Ghelder, C.V., Esmenjaud, D., 2016. TNL genes in peach: insights into the post LRR domain. BMC genomics 17 (317), 1–16.

Goldsbrough, A.P., Albrecht, H., Stratford, R., 1993. Salicylic acid-inducible binding of a tobacco nuclear protein to a 10 bp sequence which is strongly conserved amongst stress-inducible genes. Plant J. 3, 563–571.

Grant, J.J., Loake, G.J., 2000. Role of reactive oxygen intermediates and cognate redox signaling in disease resistance. Plant Physiol. 124, 21–29.

Gruber, M., Söding, J., Lupas, A.N., 2006. Comparative analysis of coiled-coil prediction methods. Struct. Biol. 155 (2), 140–145.

Guan, X., Zhao, H.Q., Xu, Y., Wang, Y.J., 2011. Transient expression of glyoxal oxidase from the Chinese wild grape *Vitis pseudoreticulata* can suppress powdery mildew in a susceptible genotype. Protoplasma 248, 415–423.

Heath, M.C., 2000. Hypersensitive response-related death. Plant Mol. Biol. 44, 321–334.

Heil, M., Baldwin, I.T., 2002. Fitness costs of induced resistance: emerging experimental support for a slippery concept. Trends Plant Sci. 7, 61–67.

Hoffmann, S., Di, Gaspero, G., Kovacs, L.G., Howard, S., Kiss, E., Galbacs, R., Testolin, R., Kozma, P., 2008. Resistance to *Erysiphe necator* in the grapevine 'Kishmish vatkana' is controlled by a single locus through restriction of hyphal growth. Theor. Appl. Genet. 116, 427–438.

Hong, Z.L., Delauney, A.J., Verma Des, PalS., 2001. A cell plate-specific callose synthase and its interaction with phragmoplastin. Plant Cell 13, 4755–4768.
Horsch, R.B., Fry, J.E., Hoffman, N.L., Einchholtz, D., Rogers, S.G., Fraley, R.T., 1985. A simple and general method for transferring genes into plants. Science 227, 1229–1231.
Jacobs, A.K., Lipka, V., Burton, R.A., Panstruga, R., Strizhov, N., Schulze-Lefert, P., et al., 2003. An*Arabidopsis* callose synthase, GSL5, is required for wound and papillary callose formation. Plant Cell 15, 2503–2513.
Jebanathirajaha, J.A., Perib, S., Pandey, A., 2002. Toll and interleukin-1 receptor (TIR) domain-containing proteins in plants: a genomic perspective. Trends Plant Sci. 7 (9), 388–391.
Jefferson, R., 1987. Assaying chimeric genes in plants: the GUS gene fusion system. Plant Mol. Biol. Rep. 5, 387–405.
Jones, J.D.G., Dangl, J.F., 2006. The plant immune system. Nature 444, 323–329.
Kajava, A.V., 1998. Structure diversity of leucine-rich repeat proteins. Mol. Biol. 277, 519–527.
Kim, S.H., Kwon, S.I., Saha, D., Anyanwu, N.C., Gassmann, W., 2009. Resistance to the *Pseudomonas syringae* effector HopA1 is governed by the TIRNBS-LRR protein RPS6 and is enhanced by mutations in SRFR1. Plant Physiol. 150, 1723–1732.
Kobe, B., Deisenhofer, J., 1994. The leucine-rich repeat: a versatile binding motif. Trends bioche. Sci. 19, 415–421.
Koch, E., Slusarenko, A., 1990. *Arabidopsis* is susceptible to infection by a downy mildew fungus. Plant Cell 2, 437–445.
Kohler, A., Schwindling, S., Conrath, U., 2000. Extraction and quantitative determination of callose from Arabidopsis leaves. Biotechniques 28, 1084–1086.
Kovtun, Y., Chiu, W.L., Tena, G., Sheen, J., 2000. Functional analysis of oxidative stress-activated mitogen-activated protein kinase cascade in plants. Proc. Natl. Acad. Sci. U.S.A. 97, 2940–2945.
Lamb, C., Dixon, R.A., 1997. The oxidative burst in plant disease resistance. Annu. Rev. Plant Physiol. Mol. Biol. 48, 251–275.
Lescot, M., Déhais, P., Thijs, G., Marchal, K., Moreau, Y., Van de Peer, Y., et al., 2002. PlantCARE, a database of plant *cis*-acting regulatory elements and aportal to tools for in silico analysis of promoter sequences. Nucleic Acids Res. 30, 325.
Li, Y.Q., Yang, S.H., Yang, H.J., Jian, H., 2007. The TIR-NB-LRR gene SNC1 is regulated at the transcript level by multiple factors. Mol. Plant Microbe Interact. 20 (11), 1449–1456.
Li, H.E., Xu, Y., Xiao, Y., Zhu, Z.G., Xie, X.Q., Zhao, H.Q., Wang, Y.J., 2010. Expression and functional analysis of two genes encoding transcription factors, *VpWRKY1* and *VpWRKY2*, isolated from Chinese wild *Vitis pseudoreticulata*. Planta 232, 1325–1337.
Lukasik-Shreepaathy, W., Slootweg, E., Richter, H., Goverse, A., Cornelissen, B.J.C., Takken, F.L.W., 2012. Dual regulatory roles of the extended N terminus for activation of the tomato Mi-1.2 resistance protein. Mol. Plant Microbe Interact. 25, 1045–1057.
Luna, E., Pastor, V., Robert, J., Flors, V., Mauch-Mani, B., Ton, J., 2011. Callose deposition: a multifaceted plant defense response. Mol. Plant Microbe Interact. 24, 183–193.
Maekawa, T., Cheng, W., Spiridon, L.N., Töller, A., Lukasik, E., Saljo, Y., et al., 2008. The Coiled-Coil and nucleotide binding domains of the potato Rx disease resistance protein function in pathogen recognition and signaling. Plant Cell 20 (3), 739–751.
Mantelin, S., Peng, H.C., Li, B.B., Atamian, H.S., Takken, F.W., Kaloshian, I., 2011. The receptor-like kinase SlSERK1 is required for Mi-1-mediated resistance to potato aphids in tomato (2013). Plant J. 67 (3), 459–471.
Mino, M., Maekawa, K., Ogawa, K., Yamagishi, H., Inoue, M., 2002. Cell death processes during expression of hybrid lethality in inter-specific F1 hybrid between *Nicotiana gossei* domain and *Nicotiana tabacum*. Plant Physiol. 130, 1776–1787.
Mittler, R., Vanderauwera, S., Gollery, M., Breusegem, F.V., 2004. Reactive oxygen gene network of plants. Trends Plant Sci. 9, 490–498.
Mohr, T.J., Mammarella, N.D., Hoff, T., Woffenden, B.J., Jelesko, J.G., et al., 2010. The *Arabidopsis* downy mildew resistance gene RPP8 is induced by pathogens and salicylic acid and is regulated by W box *cis*-elements. Mol. Plant Microbe Interact. 23, 1303–1315.
Mu, J.Y., Qian, Y.M., Ren, M., Liu, Y.H., Zhang, X.W., Wang, Z.D., Pan, Y.H., 2014. QTL analysis of resistance gene to powdery mildew in tobacco. Acta Tabacaria Sin. Acta Tab. Sin. 19 (4), 105–108.
Mukhtar, M.S., Carvunis, A.R., Dreze, M., Epple, P., Steinbrenner, J., Moore, J., et al., 2011. Independently evolved virulence effectors converge onto hubs in a plant immune system network. Science 333, 596–601.
Nandety, R.S., Caplan, J.L., Cavanaugh, K., Perroud, B., Wroblewski, T., Michelmore, R.W., et al., 2013. The role of TIR-NBS and TIR-X proteins in plant basal defense response. Plant Physiol. 162, 1459–1472.
Nie, H.Z., Wu, X.Y., Yao, C.P., Tang, D.Z., 2011. Suppression of *edr2*-mediated powdery mildew resistance, cell death and ethylene-induced senescence by mutations in ALD1 in *Arabidopsis*. Genet. Genomics 38, 137–148.
Oldroyd, G.E.D., Staskawicz, B.J., 1998. Genetically engineered broad-spectrum disease resistance in tomato. Proc. Natl. Acad. Sci. U.S.A. 95, 10300–10305.
Ooijen, G.V., Mayr, G., Albrecht, M., Cornelissen, B.J.C., Takken, F.L.W., 2008. Trans-complementation, but not physical association of the CC-NBARC and LRR domains of tomato R protein Mi-1.2 is altered by mutations in the ARC2 subdomain. Mol. Plant 1, 401–410.
Peng, H.C., Kaloshian, I., 2014. The tomato leucine-Rich repeat receptor-like kinases *SlSERK3A* and *SlSERK3B* have overlapping functions in bacterial and nematodeinnate immunity. PLoS ONE 9 (3), e93302.
Rairdan, G.J., Collier, S.M., Sacco, M.A., Baldwin, T.T., Boettrich, T., Moffett, P., 2008. The Coiled-Coil and nucleotide binding domains of the potato Rx disease resistance protein function in pathogen recognition and signaling. Plant Cell 20 (3), 739–751.
Riedl, S.J., Li, W., Chao, Y., Schwarzenbacher, R., Shi, Y., 2005. Structure of the apoptotic protease-activating factor 1 bound to ADP. Nature 434, 926–933.
Rodamilans, B., León, D.S., Mühlberger, L., Candresse, T., Neumüller, M., Oliveros, J.C., aGarcía, J.A., 2014. Transcriptomic analysis of Prunus domestica undergoing hypersensitive response to plum pox virus infection. PLoS One 9, e100477.
Santos-Rosa, M., Poutaraud, A., Merdinoglu, D., Mestre, P., 2008. Development of a transient expression system in grapevine via *agro*-infiltration. Plant Cell Rep. 27, 1053–1063.
Schenk, S.T., Schikora, A., 2015. Staining of callose depositions in root and leaf tissues. Bio-protocol 5 (6), e1429.
Shirano, Y., Kachroo, P., Shah, J., Klessig, D.F., 2002. A gain-of-function mutation in an *Arabidopsis* Toll Interleukin1 receptor-nucleotide binding site-leucine-rich repeat type R gene triggers defense responses and results in enhanced disease resistance. Plant Cell. 14 (12), 3149–3162.
Slack, J.L., Schooley, K., Bonnert, T.P., Mitcham, J.L., Qwarnstrom, E.E., Sims, J.E., Dower, S.K., 2000. Identification of two major sites in the type I interleukin-1 receptor cytoplasmic region responsible for coupling to pro-Inflammatory signaling pathways. Biol. Chem. 275 (7), 4670–4678.
Smith, L.D., Goodman, N.L., 1975. Improved culture method for the isolation of *Histoplasma capsulatum* and *Blastomyces dermatitidis* from contaminated specimens. Am. J. Clin. Pathol. 63, ,276–280.
Stokes, T.L., Kunkel, B.N., Richards, E.J., 2002. Epigenetic variation in *Arabidopsis* disease resistance. Genes Dev. 16, 171–182.
Takken, F.L.W., Goverse, A., 2012. How to build a pathogen detector: structural basis of NB-LRR function. Curr. Opin. Plant Biol. 15 (4), 375–384.
Takken, F.L.W., Albrecht, M., Tameling, W.I., 2006. Resistance proteins: molecular switches of plant defense. Curr. Opin. Plant Biol. 9 (4), 383–390.
Tang, D.Z., Innes, R.W., 2002. Over-expression of a kinase-deficient form of the EDR1gene enhances powdery mildew resistance and ethyleneinduced senescence in Arabidopsis. Plant J. 32, 975–983.
Tang, X., Xie, M., Kim, Y.J., Zhou, J., Klessig, D.F., Martin, G.B., 1999. Overexpression of *Pto* activates defense responses and confers broad resistance. Plant Cell 11, 15–29.
Torres, M.A., Jones, J.D., Dangl, J.L., 2006. Reactive oxygen species signaling in response to pathogens. Plant Physiol. 141, 373–378.
Ulker, U., Shahid, M.M., Somssich, I.E., 2007. The WRKY70 transcription factor of *Arabidopsis* influences both the plant senescence and defense signaling pathways. Planta 226, 125–137.
Wan, H.J., Yuan, W., Ye, Q.J., Wang, R.Q., Ruan, M.Y., Li, Z.M., et al., 2012. Analysis of TIR- and non-TIR-NBS-LRR disease resistance gene analogous in pepper: characterization, genetic variation, functional divergence and expression patterns. BMC Genomics 13, 502.
Wang, Y.J., Liu, Y.L., He, P.C., Chen, J., Lamikanra, O., Lu, J., 1995. Evaluation of foliar resistance to *Uncinula necatorin* Chinese wild *Vitis* species. Vitis 3, 159–164.
Wang, Y., He, P., Zhang, J., 1999. Studies on the methods of resistance to *Uncinula necatorin Vitis*. J. Northwest Sci-Tech Univ. Agric. For. 27, 6e10 (Abstract in English).
Weaver, L.M., Swiderski, M.R., Li, Y., Jone, D.G., 2006. The *Arabidopsis* thaliana TIR-NB-LRR R-protein, RPP1A; protein localization and constitutive activation of defence by truncated alleles in tobacco and *Arabidopsis*. Plant J. 47, 829–840.
Wees, S.V., 2008. Phenotypic analysis of *Arabidopsis* mutants: trypan blue stain for fungi, oomycetes, and dead plant cells. Cold Spring Harb. Protoc. 3 (8), 1–2.
Wen, Z.F., Yao, L.P., Wan, R., Li, Z., Liu, C.H., Wang, X.P., 2015. Ectopic expression in *Arabidopsis thaliana* of an NB-ARC encoding putative disease resistance gene from Wild Chinese *Vitis pseudoreticulata* enhances resistance to phytopathogenic fungi and bacteria. Front. Plant Sci. 6, 1087.
Weng, K., Li, Z.Q., Liu, Q.R., Wang, L., Wang, Y.J., Xu, Y., 2014. Transcriptome of *Erysiphe necator*-infected *Vitis* pseudoreticulata leaves provides insight into grapevine resistance to powdery mildew. Hortic. Res. 1, 14049.
Wulff, B.B., Kruijt, M., Collins, P.L., Thomas, C.M., Ludwig, A.A., De Wit, P.J., Jones, J.D., 2004. Gene shuffling-generated and natural variants of the tomato resistance gene Cf-9 exhibit different auto-necrosis-inducing activities in *Nicotiana* species. Plant J. 40, 942–956.
Xu, W.R., Yu, Y.H., Ding, J.H., Hua, Z.Y., Wang, Y.J., 2010. Characterization of a novel stilbene synthase promoter involved in pathogen- and stress-inducible expression from Chinese wild *Vitis pseudoreticulata*. Planta 231, 475–487.
Yu, Y.H., Xu, W.R., Wang, S.Y., Xu, Y., Li, H.E., Wang, Y.J., Li, S.X., 2011. VpRFP1, a novel C4C4-type RING finger protein gene from Chinese wild *Vitis pseudoreticulata*, functions as a transcriptional activator in defense response of grapevine. J. Exp. Bot. 62 (15), 5671–5682.
Yu, Y.H., Xu, W.R., Wang, J., Wang, L., Yao, W.K., Yang, Y.Z., Ma, F.L., Du, Y.J., Wang, Y.J., 2013a. The Chinese wild grapevine (*Vitis pseudoreticulata*) E3 ubiquitin ligase *Erysiphe necator*-induced RING finger protein 1 (EIRP1) activates plant defense responses by inducing proteolysis of the VpWRKY11 transcription factor. New Phytol. 200, 834–846.
Yu, Y.H., Xu, R.W., Wang, J., Wang, L., Yao, W.K., Xu, Y., Ding, J.H., Wang, Y.J., 2013b. A core functional region of the RFP1 promoter from Chinese wild grapevine is activated by powdery mildew pathogen and heat stress. Planta 237, 293–303.
Zhang, J.J., Wang, Y.J., Wang, X.P., Yang, K.Q., Yang, J.X., 2003. An improved method for rapidly extracting total RNA from *Vitis*. J. Fruit. Sci. 53, 771–787. Available on line at: http://www.gskk.cbpt.cnki.net/WKA/WebPublication/paperDigest.aspx?.

Zhang, Y., Dorey, S., Swiderski, M.S., Jones, J.D.G., 2004. Expression of *RPS4* in tobacco induces an AvrRps4-independent HR that requires *EDS1*, *SGT1* and *HSP90*. Plant J. 40 (2), 213–224.
Zhang, L., Li, Y.Z., Lu, W.J., Meng, F., Wu, C.A., Guo, X.Q., 2012. CottonGhMKK5affects disease resistance, induces HR-like cell death, and reduces the tolerance to salt and drought stress in transgenic *Nicotiana benthamiana*. J. Exp. Bot. 63 (10), 3935–3952.
Zhang, J.C., Zheng, H.Y., Li, Y.W., Li, H.J., Liu, X., Qiu, H.J., Dong, L.L., Wang, D.W., 2016. Co-expression network analysis of the genes regulated by two types of resistance responses to powdery mildew in wheat. Sci. Rep. 6, 23805.